Suppression of MYC transcription activators by the immune cofactor NPR1 fine tunes plant immune responses

Article

Cell Reports

Suppression of MYC transcription activators by the immune cofactor NPR1 fine-tunes plant immune responses

Graphical abstract

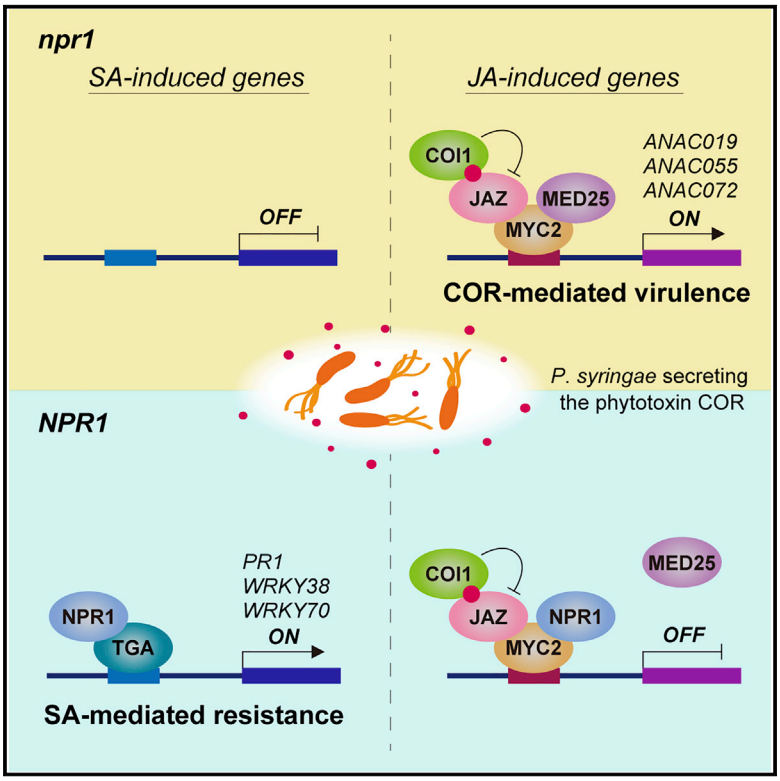

Highlights

- NPR1 physically interacts with JA-induced MYC2 and its homologs
- NPR1 is distributed to the JA-responsive promoters occupied by MYC2 and MED25
- NPR1 dissociates the MYC2-MED25 interaction to repress JA-responsive gene expression
- NPR1 suppresses MYC-mediated susceptibility of virulent *Pseudomonas syringae*

Authors

Mika Nomoto, Michael J. Skelly, Tomotaka Itaya, ..., Hironaka Tsukagoshi, Steven H. Spoel, Yasuomi Tada

Correspondence

steven.spoel@ed.ac.uk (S.H.S.), ytada@gene.nagoya-u.ac.jp (Y.T.)

In brief

Nomoto et al. demonstrate the mechanistic details of crosstalk signaling between the phytohormones salicylic acid (SA) and jasmonic acid (JA). The SA-induced immune cofactor NPR1 directly inhibits JA-induced MYC activators, suppressing the virulent effect of the phytotoxin coronatine (COR) secreted from *Pseudomonas syringae*.

Nomoto et al., 2021, Cell Reports *37*, 110125
December 14, 2021
https://doi.org/10.1016/j.celrep.2021.110125

CellPress

Cell Reports

CellPress
OPEN ACCESS

Article

Suppression of MYC transcription activators by the immune cofactor NPR1 fine-tunes plant immune responses

Mika Nomoto,[1,2] Michael J. Skelly,[3] Tomotaka Itaya,[1] Tsuyoshi Mori,[1] Takamasa Suzuki,[4,5] Tomonao Matsushita,[6] Mutsutomo Tokizawa,[7] Keiko Kuwata,[8] Hitoshi Mori,[9] Yoshiharu Y. Yamamoto,[7] Tetsuya Higashiyama,[1,4,8] Hironaka Tsukagoshi,[10] Steven H. Spoel,[3,*] and Yasuomi Tada[1,2,11,*]

[1]Division of Biological Science, Graduate School of Science, Nagoya University, Chikusa, Nagoya, Aichi 464-8602, Japan
[2]Center for Gene Research, Nagoya University, Chikusa, Nagoya, Aichi 464-8602, Japan
[3]Institute of Molecular Plant Sciences, School of Biological Sciences, University of Edinburgh, Edinburgh EH9 3BF, UK
[4]JST ERATO Higashiyama Live-Holonics Project, Nagoya University, Chikusa, Nagoya, Aichi 464-8602, Japan
[5]College of Bioscience and Biotechnology, Chubu University, Aichi 487-8501, Japan
[6]Graduate School of Science, Kyoto University, Sakyo, Kyoto 606-8502, Japan
[7]Faculty of Applied Biological Sciences, Gifu University, Gifu 501-1193, Japan
[8]Institute of Transformative Bio-Molecules (WPI-ITbM), Nagoya University, Chikusa, Nagoya, Aichi 464-8602, Japan
[9]Graduate School of Agriculture, Nagoya University, Chikusa, Nagoya, Aichi 464-8601, Japan
[10]Faculty of Agriculture, Meijo University, Tenpaku, Nagoya, Aichi 468-8502, Japan
[11]Lead contact
*Correspondence: steven.spoel@ed.ac.uk (S.H.S.), ytada@gene.nagoya-u.ac.jp (Y.T.)
https://doi.org/10.1016/j.celrep.2021.110125

SUMMARY

Plants tailor immune responses to defend against pathogens with different lifestyles. In this process, antagonism between the immune hormones salicylic acid (SA) and jasmonic acid (JA) optimizes transcriptional signatures specifically to the attacker encountered. Antagonism is controlled by the transcription cofactor NPR1. The indispensable role of NPR1 in activating SA-responsive genes is well understood, but how it functions as a repressor of JA-responsive genes remains unclear. Here, we demonstrate that SA-induced NPR1 is recruited to JA-responsive promoter regions that are co-occupied by a JA-induced transcription complex consisting of the MYC2 activator and MED25 Mediator subunit. In the presence of SA, NPR1 physically associates with JA-induced MYC2 and inhibits transcriptional activation by disrupting its interaction with MED25. Importantly, NPR1-mediated inhibition of MYC2 is a major immune mechanism for suppressing pathogen virulence. Thus, NPR1 orchestrates the immune transcriptome not only by activating SA-responsive genes but also by acting as a corepressor of JA-responsive MYC2.

INTRODUCTION

Plants have developed sophisticated innate immune responses similar to those found in insects and humans as well as plant-specific immune systems (Spoel and Dong, 2012). Upon infection with biotrophic pathogens that feed on living host cells, intracellular immune receptors directly or indirectly recognize pathogen-secreted effector proteins to trigger the hypersensitive response, which includes a form of programmed cell death, oxidative burst, and callose deposition, to sequester pathogens at the site of infection (Dangl and Jones, 2001; Dodds and Rathjen, 2010; Jones and Dangl, 2006). Furthermore, the infected tissues produce systemic signals, such as methyl salicylic acid, azelaic acid, a lipid transfer protein, and pipecolic acid (Hartmann et al., 2018; Jung et al., 2009; Maldonado et al., 2002; Park et al., 2007), that initiate distal accumulation of the immune hormone salicylic acid (SA). SA induces transcriptional reprogramming, including expression of antimicrobial pathogenesis-related (*PR*) genes, inhibiting pathogen growth and spread. This immune response is known as systemic acquired resistance (SAR) and has been demonstrated to provide long-lasting and broad-spectrum resistance to biotrophs (Fu and Dong, 2013).

Perception of SA is mediated by a nuclear receptor complex that contains the transcriptional coactivator NONEXPRESSOR OF *PR* GENES 1 (NPR1) (Cao et al., 1997; Fu et al., 2012; Manohar et al., 2015; Wu et al., 2012). The NPR1 coactivator directly interacts with members of the TGACG-binding factor (TGA) family of basic leucine zipper (bZIP) transcription factors to activate expression of myriad immune genes, including *PR* genes (Saleh et al., 2015; Spoel and Dong, 2012; Tada et al., 2008). SA regulates recruitment of NPR1 to its paralogs NPR3 and NPR4, which function as substrate adaptors for a Cullin3-RING ubiquitin ligase ($CRL3^{NPR3/4}$), resulting in ubiquitin-mediated control of NPR1 transcriptional activity (Fu et al., 2012; Skelly et al., 2019; Spoel et al., 2009). Accordingly, mutation of NPR1 protein

results in SA insensitivity, failure to reprogram gene transcription upon pathogen attack, and extreme susceptibility to biotrophs (Wang et al., 2006).

In addition to defenses against biotrophs, plants have developed different immune responses against necrotrophic pathogens that kill host cells before feeding. Necrotrophic pathogen attack leads to rapid accumulation of jasmonic acid (JA), which is perceived through a nuclear receptor complex consisting of the F-box protein CORONATINE INSENSITIVE 1 (COI1) and members of the JASMONATE ZIM DOMAIN (JAZ) family of transcriptional cofactors (Chini et al., 2007; Katsir et al., 2008; Sheard et al., 2010; Thines et al., 2007; Yan et al., 2007). In the absence of JA, JAZ cofactors competitively inhibit transcription activators of JA-responsive genes, including the basic-helix-loop-helix (bHLH) transcription factors MYC2, MYC3, and MYC4, by preventing their interaction with the MED25 subunit of the Mediator complex (Fernández-Calvo et al., 2011; Zhang et al., 2015). COI1 is part of a Skp-Cullin-F-box ubiquitin ligase (SCF^{COI1}) that upon binding of biologically active JA, recruits JAZ cofactors, leading to their polyubiquitination and subsequent proteasome-mediated degradation (Chini et al., 2007; Devoto et al., 2002; Xu et al., 2002). This allows MYC activators to form a transactivation complex by direct association with MED25, which recruits histone acetyltransferase1 (HAC1) and the RNA polymerase II general transcription machinery (An et al., 2017; Zhai et al., 2020). Failure to degrade JAZ cofactors in *coi1* mutants results in JA insensitivity and increased susceptibility to attack by necrotrophs (Howe and Jander, 2008; Xie et al., 1998). Similarly, *jai3-1* mutants and transgenic *35S:JAI3-ΔC* plants, which produce a truncated form of JAZ3 protein resistant to SCF^{COI1}-mediated degradation, also exhibit JA insensitivity (Chini et al., 2007).

Antagonism between SA and JA signaling has been reported extensively and allows plants to fine-tune immune responses according to the attacker encountered. For example, the biotrophic pathogen *Pseudomonas syringae* pv. *tomato* (*Pst*) employs a virulence strategy that involves production of the toxin coronatine (COR), a mimic of biologically active JA that functions as a suppressor of SA-mediated defenses (Bender et al., 1999; Brooks et al., 2005; Geng et al., 2014). To counter this effect, plants have evolved mechanisms to block COR-induced JA signaling and prevent associated disease susceptibility (Howe et al., 2018). In *Arabidopsis*, SA-induced NPR1 not only initiates SA-responsive gene expression but also functions as a potent suppressor of JA-responsive gene expression (Caarls et al., 2015; Pieterse et al., 2009; Spoel et al., 2003). Consequently, upon infection with *Pst*, mutant *npr1* plants display impaired SA-responsive transcriptional reprogramming but enhanced JA-responsive gene expression. Moreover, NPR1 spatially regulates antagonism between SA and JA signals when derived from concomitant infections by biotrophs and necrotrophs, maximizing the plant's ability to defend against multiple attackers (Spoel et al., 2007). Nonetheless, little is known about the molecular mechanisms by which NPR1 functions as a negative regulator of JA-responsive genes.

Here we determined the genome-wide distribution of SA-induced NPR1 and demonstrate that it associates with JA-responsive promoters. When SA signaling is activated, chromatin occupancy of NPR1 coincided with a JA-responsive transcriptional complex consisting of MYC2 transcription factors and MED25 Mediator. Indeed, SA-induced NPR1 physically interacted with MYC2 and effectively replaced JA-regulated JAZ repressors to continue to suppress JA-responsive genes by disrupting the interaction between MYC2 and the MED25 Mediator subunit. Our findings finally shed light on the mechanisms of crosstalk between SA and JA signals and underline the importance of versatile interactions between nuclear receptor components in shaping the outcome of plant immune responses.

RESULTS

The NPR1 cofactor interacts with MYC activators at JA-responsive promoters

Although NPR1 functions as a coactivator of SA-responsive genes through direct interaction with TGA transcription factors (Després et al., 2000; Fan and Dong, 2002), it strongly suppresses JA-responsive genes by still unknown mechanisms (Spoel et al., 2003). To better understand the role of SA-induced NPR1 in suppressing JA-responsive genes, we performed RNA sequencing (RNA-seq) analysis on 2-week-old *Arabidopsis* wild-type Columbia (Col-0) and mutant *npr1-3* plants treated for 24 h with methyl-JA (MeJA) or a combination of SA and MeJA. Among 1,774 JA-induced genes, 289 genes were differentially downregulated by SA in an NPR1-dependent manner (Table S1; Figures S1A and S1B), indicating that NPR1 suppresses a specific subset of JA-responsive genes. We then performed a comparative and unbiased analysis of the promoter sequences of these 289 genes, which determines statistically enriched octamer sequences (Yamamoto et al., 2011). As shown in Figure S1C, this analysis revealed enrichment of G-box motifs that were statistically highly overrepresented, implying that 289 genes are controlled by MYC2 and JAZ transcriptional regulators. Although we also found enrichment of G-box motifs in 207 genes that are suppressed by SA but not by NPR1 (Table S1; Figures S1A and S1D), Gene Ontology (GO) analysis by the PANTHER classification system indicated that the 289 genes downregulated in an NPR1-dependent manner were differentially enriched for responses related to JA, defense, and insects (Table S1; Figure S1E). Therefore, although these two gene sets possess the same G-box motifs, they are regulated by a different combination of transcription factors.

Previous work has shown that, after co-treatment with SA and JA, JAZ repressors are still eliminated (Van der Does et al., 2013), so why do MYC activators fail to induce JA-responsive gene expression under these conditions? We hypothesized that SA-induced NPR1 may act as a substitute for JAZ repressors to form a transcriptional repressor complex at JA-responsive promoters. It has been reported previously that NPR1 may suppress JA signaling from the cytoplasm (Spoel et al., 2003). Nonetheless, we observed that, similar to SA treatment alone, co-treatment with SA and JA resulted in normal accumulation of NPR1-GFP in the nucleus (Figure S1F), leaving open the possibility that nuclear NPR1 also plays a role in suppression of JA-responsive genes. Thus, we surveyed the genome-wide distribution of NPR1 in the presence of SA and JA by chromatin immunoprecipitation sequencing (ChIP-seq) of NPR1-GFP-expressing

seedlings. The correlation matrix of the read coverages between three biological replicates (rep1–rep3) indicated high reproducibility (Figure S1G). Plotting of the average occupancy profile in relation to gene bodies identified a single peak that mapped to positions directly upstream of the transcription start site (TSS) (Figure 1A). By comparing immunoprecipitation (IP) using an anti-GFP antibody with a pre-immune serum (input), model-based analysis of ChIP-seq (MACS2) determined, respectively, 5,442, 4,304, and 4,955 NPR1-binding peaks in the three replicates (Table S2; $p < 0.05$ and score > 30). At least 74% of NPR1-binding peaks were located in the promoter regions for each replicate (Figure 1B; Figure S1H). Based on the common profiles of NPR1-binding peaks in three biological replicates, we extracted 2,554 NPR1-targeted genes (Table S2; Figure 1C). GO analysis indicated that these 2,554 genes were enriched not only for responses related to SA but also to JA, suggesting that NPR1 localizes to the promoters of JA-responsive genes (Figure 1D). To identify specific DNA sequences to which NPR1 is recruited, we performed *de novo* motif analysis of NPR1-binding peaks with multiple expectation maximizations (ME) for motif elicitation (MEME)-ChIP, using the read sequences of the 2,554 genes. Not only did we identify TGACG motifs that are bound by SA-responsive TGA transcription factors known to interact with NPR1, again we found significant enrichment of G-box motifs (CACGTG) (Figure 1E; Figure S1I). Although we also found enrichment of C-box motifs for basic pentacysteine (BPC) transcription factors in all replicates (Petrella et al., 2020), there is no evidence that BPCs directly regulate JA-responsive gene expression. Thus, our results suggest that NPR1 may form a transcriptional repressor complex that inhibits the activity of MYC activators at JA-responsive promoters.

To investigate whether NPR1 directly targets MYC2 and its homologs, we performed *in vitro* protein-protein interaction assays using recombinant biotin acceptor peptide (BAP)-tagged NPR1 (NPR1-BAP), JAZ1-BAP, and FLAG-tagged MYC proteins. Similar to the previously reported interaction between JAZ1 and MYC proteins (Figure 2A, right panel; Figure S2A; Fernández-Calvo et al., 2011), NPR1 also strongly interacted with MYC2, MYC3, and MYC4 (Figure 2A, left panel; Figures S2A and S2B). We then questioned whether NPR1 binds to the N-terminal region of MYC2, containing the JAZ-interacting domain (JID) and transcription activation domain (TAD), which are utilized by JAZ and MED25 proteins to halt and activate MYC2-dependent transcription, respectively. As shown in Figure 2B, deletion of the N-terminal region completely abolished the *in vitro* interaction between NPR1 and MYC2. This was further validated by pull-down assays demonstrating that the interaction of FLAG-JAZ1 with hemagglutinin (HA)-tagged MYC2 (MYC2-HA) was competitively reduced by NPR1-BAP in a dose-dependent manner (Figure 2C).

To confirm NPR1-MYC interactions *in vivo*, bimolecular fluorescence complementation (BiFC) assays were performed in *Nicotiana benthamiana* leaves and *Arabidopsis* Col-0 protoplast cells. The N-terminal half of yellow fluorescent protein (YFP) was fused to MYC2, MYC3, and MYC4 (nYFP-MYCs), whereas the C-terminal half was fused to NPR1 (NPR1-cYFP). Strong fluorescence was detected in *N. benthamiana* and *Arabidopsis* nuclei when NPR1-cYFP and nYFP-MYCs were transiently coexpressed (Figure 2D; Figure S2C). In addition, coIP experiments were carried out using transgenic plants expressing *pMYC2:MYC2-FLAG* in the *jin1-8/myc2* (Figure S2D) and *npr1-3* backgrounds to further verify *in vivo* interaction. As shown in Figure 2E, we confirmed that treatment with SA or SA/MeJA clearly facilitated association of NPR1 with MYC2. These data support the notion that SA-induced NPR1 protein forms a complex with MYC activators at JA-responsive promoters. Importantly, because activation of the SA and JA signaling pathways eliminates JAZ proteins (Van der Does et al., 2013), NPR1 probably does not compete with JAZ proteins for interaction with MYC2 but, rather, substitutes their repressor function.

Transcriptionally active MYC2-mediator complexes attract NPR1 to JA-responsive promoters

MYC2 activates JA-responsive genes by interacting with MED25, a subunit of the Mediator transcriptional coactivator complex, which stimulates promoter looping between JA enhancers and their promoters (Wang et al., 2019). Thus, occupancy of promoters by both MYC2 and MED25 is a proxy for actively transcribed JA-responsive genes. To investigate whether NPR1 targets MYC2 at actively transcribed JA-responsive genes, we compared the genome-wide occupancy pattern of SA/MeJA-induced NPR1 with that of MYC2/MED25. We found that 45.2% of reported MYC2 and MED25 co-targeted genes were also occupied by NPR1 (1,137 of 2,514) (Table S2; Figure 3A). These 1,137 genes were significantly enriched for GO terms associated with regulation by the JA-mediated signaling pathway as well as for response to SA (Figure 3B), whereas MEME-ChIP analysis identified G-box and TGACG motifs as overrepresented sequences (Figure 3C). Using the Integrative Genomics Viewer (IGV) browser (Thorvaldsdóttir et al., 2013), we then visualized the binding site distribution of NPR1 and MYC2/MED25. As shown in Figure 3D, NPR1 was enriched at promoter regions of the SA-responsive marker genes *PR1*, *WRKY38*, and *WRKY70*, all of which contain TGACG motifs. As expected, binding of MYC2/MED25 to these promoters was absent or very low. In contrast, promoters of the JA-responsive marker genes *JAZ8*, *JAZ9*, and *JRG21* and other JA-responsive genes showed clear co-occupancy by MYC2/MED25 (Figure 3E; Figure S3A). Surprisingly, we found that, at these genes, NPR1 exhibited the same binding distribution as MYC2/MED25 and preferentially bound at G-box motifs rather than at TGACG motifs (Figure 3E; Figure S3A). These results indicate that SA exerts its negative effect on JA signaling through recruitment of NPR1 to MYC2/MED25-occupied promoter regions of JA-responsive genes.

So how is SA-induced NPR1 recruited to JA-responsive promoters? We considered that MYC2 may act as a beacon that attracts NPR1. To test this hypothesis, we performed ChIP-qPCR on plants expressing *NPR1-GFP* in a *jin1-2* mutant background that lacks functional MYC2 protein (Figure S3B). As expected, SA-induced NPR1-GFP bound to the promoter of SA-responsive *PR1* regardless of the presence of a functional *MYC2* allele (Figure 3F). In contrast, SA stimulated binding of NPR1-GFP to JA-induced *LOX2*, *JRG21*, and *JAZ6* promoters, but only in the presence of functional MYC2 (Figure 3G; Figures S3C and S3D). This effect was specific to JA-responsive genes that are targeted by SA because enrichment of NPR1 at the

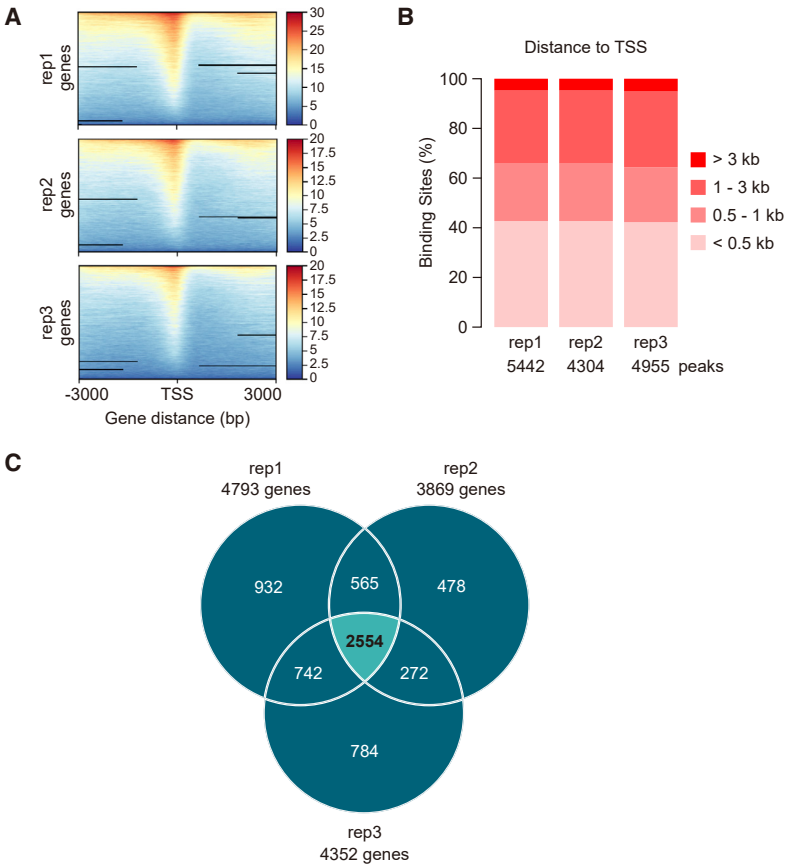

Figure 1. The SA-responsive NPR1 cofactor targets the G-box in JA signaling

(A) The correlation matrix of the read coverages for ChIP-seq experiment was visualized with plotHeatmap. TSS, transcription start site.

(B) Distribution of the distance to the nearest TSS for NPR1-binding peaks ($p < 0.05$ and score > 30).

(C) Venn diagram depicting the overlap between three biological replicates of NPR1-targeted genes determined by ChIP-seq.

(D) Enriched GO terms derived from 2,554 NPR1-targeted genes by the PANTHER classification system. Fold enrichment ($p < 0.05$) was determined by query gene number divided by expected gene number in each GO term.

(E) NPR1-binding motifs were identified *de novo* using MEME-ChIP with the corresponding *E* value in 2,554 genes. The *E* value is an estimate of the expected number of motifs that can be found in a similarly sized set of random sequences.

See also Figure S1 and Table S2.

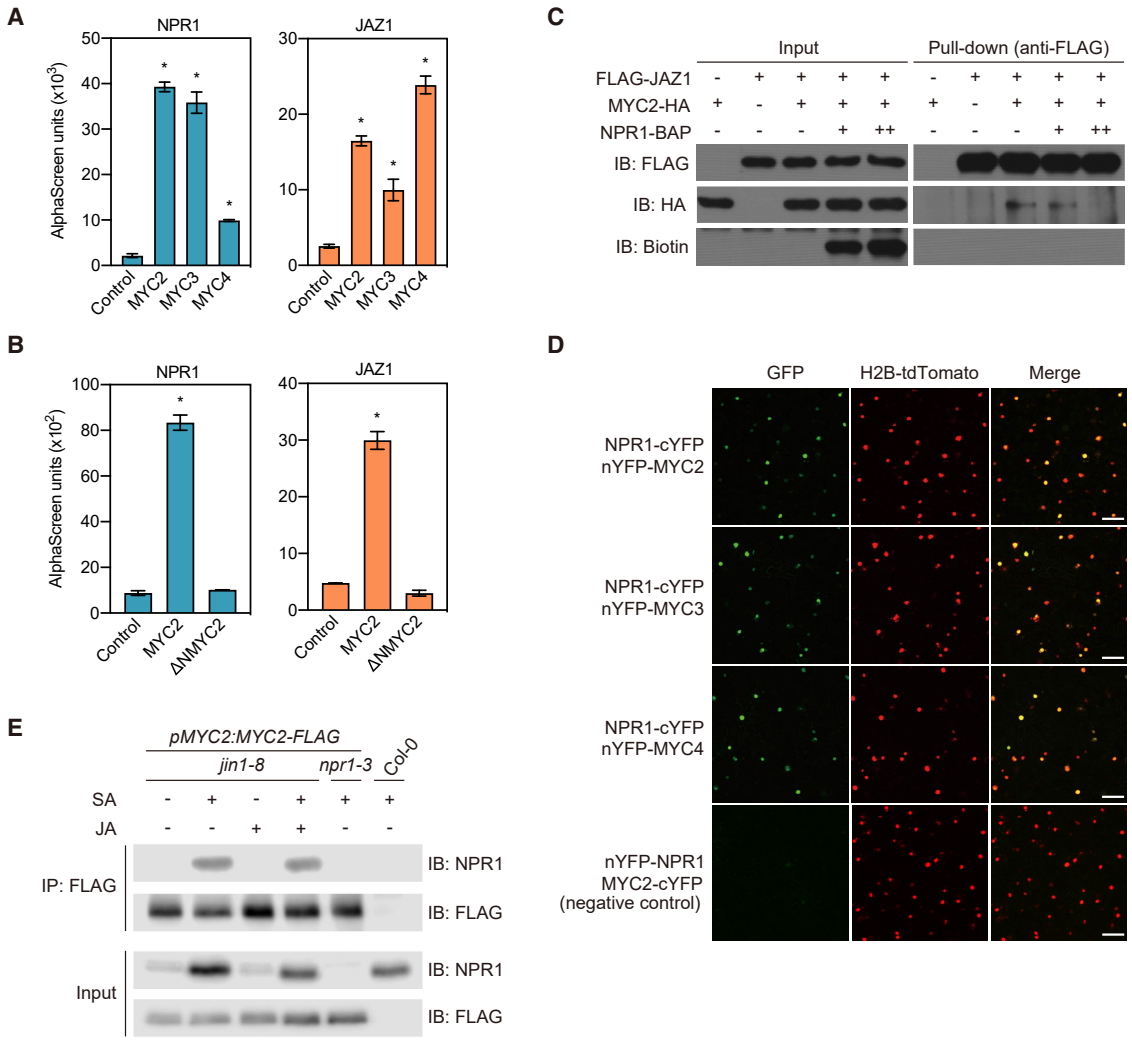

Figure 2. NPR1 cofactor interacts with MYC2 and its homologs

(A and B) *In vitro* interaction of NPR1-BAP or JAZ1-BAP with MYC2/4-FLAG, FLAG-MYC3, or ΔNMYC2-FLAG was evaluated by AlphaScreen. Control values were obtained using the uninduced *in vitro* translation mixture. Error bars indicate SE of the mean (n = 3). Asterisks indicate significant difference compared with the control (one-way ANOVA, *p < 0.001).

(C) An *in vitro* competition assay was performed using FLAG-JAZ1, MYC2-HA, and NPR1-BAP. Proteins were pulled down with an anti-FLAG antibody and detected by western blotting with anti-FLAG and anti-HA antibodies and NeutrAvidin-horseradish peroxidase (HRP). +, addition of the indicated protein; ++, double amount of protein used; –, absence of the protein.

(D) BiFC analyses were performed in *N. benthamiana* leaves 3 days after transformation with the indicated constructs. GFP, histone H2B-tdTomato, and merged signals are shown. Scale bars, 75 μm.

(E) *In vivo* interaction of MYC2-FLAG with endogenous NPR1. Two-week-old *pMYC2:MYC2-FLAG/jin1-8* seedlings were pretreated with water (mock) or 0.5 mM SA for 12 h, followed by treatment with water, 0.5 mM SA, 50 μM MeJA, or 0.5 mM SA and 50 μM MeJA for 4 h. Proteins were pulled down with an anti-FLAG antibody and detected by western blotting with anti-FLAG and anti-NPR1 antibodies.

See also Figure S2.

JA-responsive but SA-insensitive promoters of *JAV1* and *WRKY75* was not dependent on MYC2 (Figure S3E). Thus, MYC2 is the major determinant for recruitment of SA-induced NPR1 to JA-responsive genes.

NPR1 inhibits JA-responsive genes by disrupting MYC2-mediated recruitment of Mediator

Because MYC2 activity results in recruitment of NPR1 to JA-responsive genes and the two proteins physically associate *in vivo*, we sought to determine whether and how NPR1 inhibits MYC2 transcriptional activator activity. First we investigated whether JA-responsive gene expression remains dependent on MYC activators in the absence of functional NPR1 protein because this could suggest that NPR1 directly targets MYC proteins. Consistent with previous findings (Spoel et al., 2003), co-treatment of the *npr1-3* mutant with SA and MeJA failed to suppress induction of JA-responsive *VSP2*, *JAZ9*, and *LOX2* (Figure 4A). However, in *myc2 myc3 myc4 npr1-3* quadruple

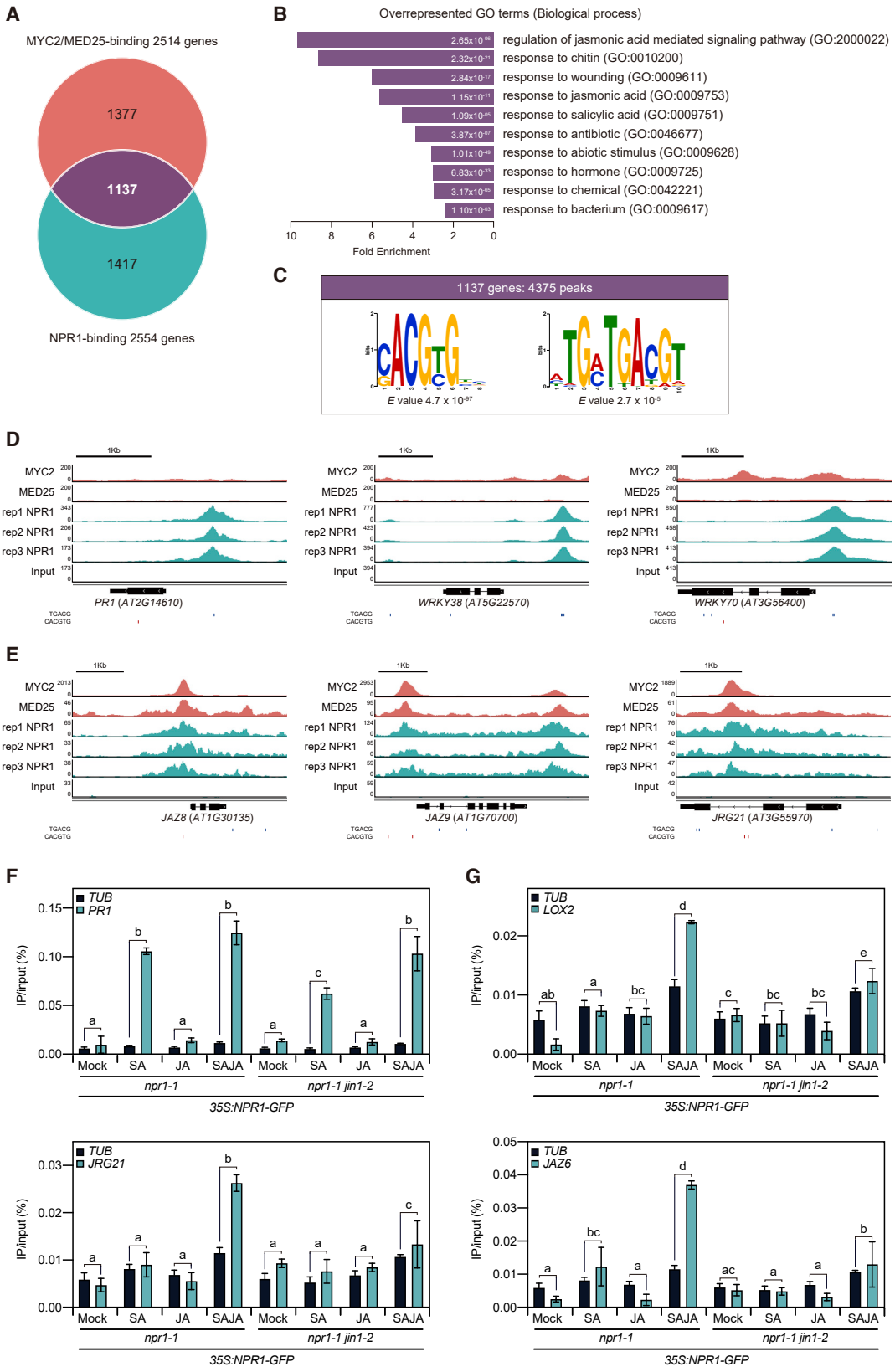

(legend on next page)

mutants (Figure S4), the expression levels of these genes were reduced to those of *myc2 myc3 myc4* triple mutants, suggesting that NPR1 indeed significantly suppressed the transcriptional activity of MYC activators.

Because NPR1 unambiguously localized to MYC2 chromatin binding sites in the presence of SA and MeJA (Figures 3E and 3G; Figures S3A and S3D), we investigated whether NPR1 suppresses accumulation of MYC2 protein and/or reduces the DNA-binding activity of MYC2. As shown in Figure 2E, SA treatment did not decrease the protein levels of constitutively expressed MYC2-FLAG in the *jin1-8/myc2* background (Hou et al., 2010), suggesting that NPR1 does not facilitate the degradation of MYC2 protein. Therefore we evaluated the enrichment of MYC2-FLAG at JA-responsive promoters after co-treatment with SA and MeJA. Compared with mock or SA-treated tissues, treatment with MeJA alone significantly enhanced recruitment of MYC2-FLAG to the *JAZ6*, *JAZ9*, *LOX2*, *LOX3*, *LOX4*, and *JRG21* promoters (Figure 4B). Likewise, simultaneous treatment with SA and MeJA still resulted in normal recruitment of MYC2-FLAG to these promoters, indicating that NPR1 does not hinder the DNA-binding activity of MYC activators.

Our findings suggest that NPR1 may directly inhibit the transcriptional activity of MYC2 at JA-responsive promoters. To test this, the effect of NPR1 on the transcriptional activity of MYC2 was examined, using a reporter construct consisting of the *LOX3* promoter fused to the firefly *luciferase* (*LUC*) gene (*pLOX3:fLUC*) (Figure 5A). Effector constructs of *MYC2-GFP*, *JAZ1-FLAG*, and *NPR1-FLAG* were expressed under the control of the *mannopine synthase* (*mas*) promoter from *Agrobacterium tumefaciens*, and a free *GFP* construct was used as a control. When the *pLOX3:fLUC* reporter was transiently coexpressed with *MYC2-GFP* in *N. benthamiana* leaves, LUC activity was highly induced compared with the control (Figure 5B; Figure S5A). As expected, coexpression of *JAZ1-FLAG* with *MYC2-GFP* completely abolished reporter gene activity. More importantly, NPR1 was equally capable of suppressing MYC2-GFP transcriptional activity, whereas introduction of the *npr1-1* mutation (H334Y) completely removed this repressive effect (Figure 5B; Figure S5B). Next we investigated whether NPR1 negates the positive function of MED25 in MYC2-dependent transcription using the same reporter system. When *MED25-GFP* and *MYC2-GFP* were coexpressed in *N. benthamiana* leaves, the activity of *pLOX3:fLUC* was significantly higher compared with expression of only *MYC2-GFP* (Figures 5A and 5C). Remarkably, the positive effect of MED25 on MYC2-mediated LUC activity was strongly repressed by coexpression of NPR1 or JAZ1. Next we investigated whether SA affects accumulation of MED25 at MYC2-binding regions using *35S:MED25-GFP* plants (Figure 5D). Treatment with MeJA for 20 min clearly induced MED25 binding to the promoters of *JRG21*, *JAZ6*, and *JAZ8*, whereas co-treatment with SA and MeJA abolished its accumulation. These data indicate that NPR1 suppresses JA-responsive genes by forming a repressor complex with MYC activators at G-box motifs, which prevents MYC2-mediated recruitment of Mediator.

NPR1 prevents MYC2/3/4-mediated susceptibility to virulent *Pseudomonas syringae*

Next we questioned what the biological significance is of NPR1-mediated suppression of MYC2 activity. The biotrophic pathogen *Pseudomonas syringae* pv. *maculicola* (*Psm*) ES4326 induces SA-mediated immunity in plants, but it produces the JA-mimicking phytotoxin COR, which exerts its virulence by hijacking JA signaling to suppress SA-responsive immunity (Brooks et al., 2005). It has been demonstrated that COR induces expression of the three NAM, ATAF, and CUC (NAC) transcription factors, *ANAC019*, *ANAC055*, and *ANAC072*, in a MYC2-dependent manner (Zheng et al., 2012). These three homologous genes play an important role in promoting pathogen virulence by suppressing accumulation of SA and reopening stomata to facilitate bacterial entry into leaf tissues. Thus, crosstalk between SA and COR-induced JA signaling pathways is thought to determine the degree of susceptibility to *Psm* ES4326. Therefore, we utilized *Psm* ES4326 to determine how the suppressive effect of NPR1 on MYC2 activity affects immunological outcomes. Wild-type plants and *myc2 myc3 myc4* triple, *npr1-3* single, and *myc2 myc3 myc4 npr1-3* quadruple mutants were infected with *Psm* ES4326, and disease symptoms and pathogen growth were monitored. Compared with the wild type, disruption of JA signaling in *myc2 myc3 myc4* triple mutants enhanced resistance to *Psm* ES4326 (Figure 6A), indicating that COR produced by this pathogen boosts virulence through the host MYC signaling pathway. In contrast, *npr1-3* mutants displayed enhanced disease susceptibility, but, surprisingly, this was completely abolished by introducing *myc2 myc3 myc4* mutant alleles. Because these data suggest that NPR1-mediated suppression of MYC2 activity is a major immune mechanism for suppressing pathogen virulence, we examined the transcriptional activity of SA- and JA-responsive genes during infection (Figure 6B; Figure S6). Indeed, compared

Figure 3. NPR1 localizes on JA-responsive promoters occupied by MYC2 and MED25

(A) Venn diagram depicting MYC2/MED25 and NPR1 target genes determined by ChIP-seq.

(B) Enriched GO terms derived from 1,137 NPR1/MYC2/MED25-targeted genes by the PANTHER classification system. Fold enrichment ($p < 0.05$) was determined by query gene number divided by expected gene number in each GO term.

(C) MYC2/MED25 and NPR1-binding motifs were identified *de novo* using MEME-ChIP with the corresponding *E* value in 1,137 genes.

(D) Localization of NPR1 on the SA-responsive *PR1*, *WRKY38*, and *WRKY70* promoters obtained from 1,417 genes shown in (A). Blue and red lines indicate TGACG and CACGTG (G-box) motifs, respectively.

(E) Co-occupancy of NPR1 and MYC2/MED25 on the JA-responsive *JAZ8*, *JAZ9*, and *JRG21* promoters obtained from 1,137 genes shown in (A). Blue and red lines indicate TGACG and CACGTG (G-box) motifs, respectively.

(F and G) ChIP-qPCR analyses of NPR1-GFP binding to the TGACG and G-box from *pPR1*, *pLOX2*, *pJRG21*, and *pJAZ6*. Two-week-old seedlings of *35S:NPR1-GFP* in *npr1-1* and *npr1-1 jin1-2* plants were treated with water (mock), 0.5 mM SA, 50 μM MeJA, or 0.5 mM SA and 50 μM MeJA for 6 h. Error bars represent SD ($n = 3$). Letters indicate statistically significant differences (two-way ANOVA, $p < 0.05$). The experiment was performed twice with similar results (Figures S3C and S3D).

See also Figure S3 and Table S2.

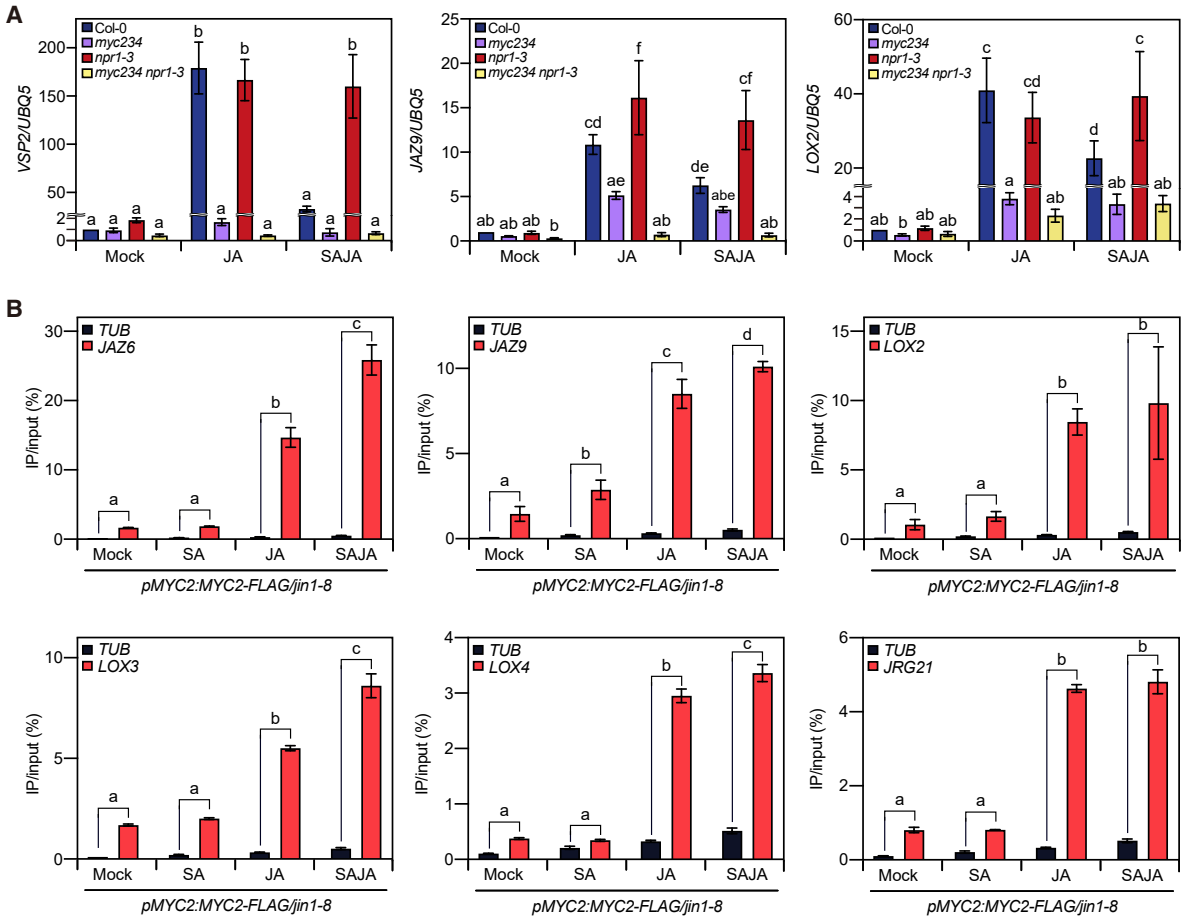

Figure 4. SA does not decrease MYC2 binding to the JA-responsive promoters

(A) Two-week-old seedlings of the indicated genotypes were treated with water (mock), 50 μM MeJA, or 0.5 mM SA and 50 μM MeJA for 6 h. Expression of *VSP2*, *JAZ9*, and *LOX2* was determined by qPCR and normalized with *UBQ5*. Error bars represent SD (n = 3). Letters indicate statistically significant differences (one-way ANOVA, $p < 0.05$).

(B) ChIP-qPCR analysis of binding of MYC2-FLAG to the G-box motif from the JA-responsive *pJAZ6*, *pJAZ9*, *pLOX2*, *pLOX3*, *pLOX4*, and *pJRG21*. Two-week-old *pMYC2:MYC2-FLAG/jin1-8* seedlings were pretreated with water (mock) or 0.5 mM SA for 12 h, followed by treatment with water, 0.5 mM SA, 50 μM MeJA, or 0.5 mM SA and 50 μM MeJA for 4 h. Error bars represent SD (n = 3). Letters indicate statistically significant differences (two-way ANOVA, $p < 0.05$). The experiment was performed twice with similar results.

See also Figure S4.

with the wild type, *Psm* ES4326 infection enhanced expression levels of JA-responsive *VSP2*, *LOX2*, *LOX3*, *JAZ8, JAZ9*, *ANAC019*, *ANAC055*, and *ANAC072* in the *npr1-3* mutant (Figure 6B). This effect was dependent on MYC activators because enhanced induction was completely lost in *myc2 myc3 myc4 npr1-3* quadruple mutants. These data indicate that NPR1 negatively regulates the transcriptional activity of MYC activators to alleviate COR-induced pathogenicity. Importantly, disease-resistant *myc2 myc3 myc4 npr1-3* quadruple mutants did not exhibit enhanced expression of SA marker genes or genes associated with pattern-triggered immunity (Figure S6), supporting the notion that NPR1-mediated suppression of JA signaling is sufficient to establish resistance to *Psm* ES4326. Hence, our results demonstrate that transcriptional suppression of MYC activators by NPR1 is a major immune mechanism for preventing hijacking of hormone signaling and limiting pathogen virulence.

DISCUSSION

NPR1 is a potent coactivator of SA-responsive gene expression (Fu and Dong, 2013). It has also been proposed to function as a corepressor of JA-responsive genes through cytoplasmic and nuclear functions, but the associated mechanisms remain unknown (Pieterse et al., 2009). JA-responsive gene expression is controlled by JAZ repressors that effectively inactivate MYC activity by binding to the N-terminal region containing the JID and TAD. JA initiates SCF^{COI1}-mediated degradation of JAZ repressors to release MYC2 activity (Kazan and Manners, 2013), resulting in activation of the JA-responsive hierarchical transcription cascade to appropriately respond to wounding and pathogen attack (Du et al., 2017). Here we found that SA-induced NPR1 forms two functionally distinct complexes with TGA and MYC activators on TGACG and G-box motifs, respectively (Figures 1 and

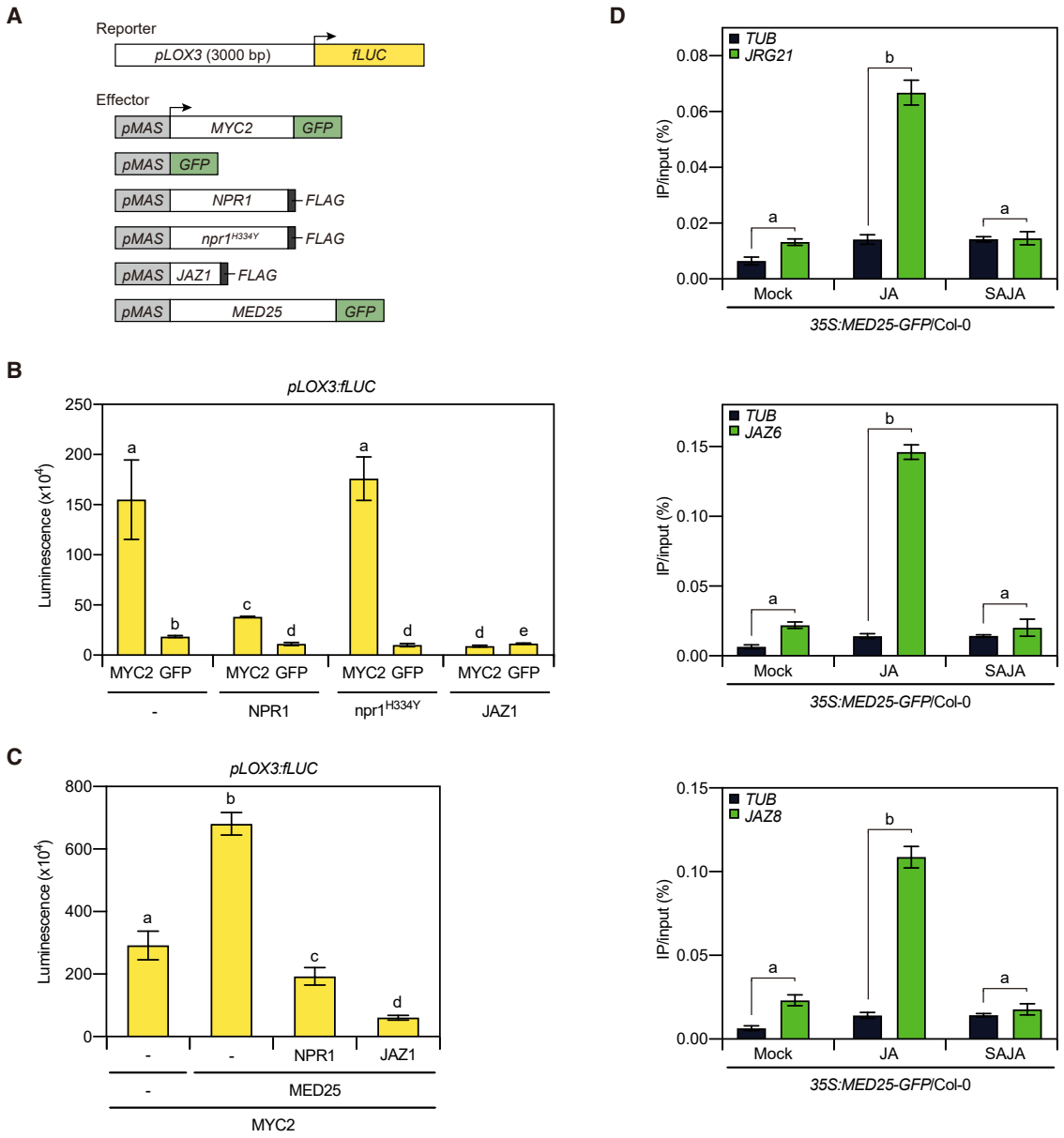

Figure 5. NPR1 directly inhibits MYC2/MED25-dependent transcriptional activity

(A) Schematic of the reporter and effectors used in the *Agrobacterium*-mediated transient assay in *N. benthamiana* leaves. *fLUC*, firefly luciferases; *pMAS*, mannopine synthase promoter.

(B) Effect of NPR1 and npr1^{H334Y} on the transcriptional activity of MYC2. Five-week-old *N. benthamiana* leaves were inoculated with *Agrobacterium* carrying the indicated constructs and incubated for 48 h. Luciferase activity was measured from protein extracts of the leaf samples. Error bars represent SD (n = 3). Letters indicate statistically significant differences (one-way ANOVA, $p < 0.05$). –, inoculation with *Agrobacterium* carrying the empty vector.

(C) Effect of NPR1 on transcriptional activity of the MYC2-MED25 complex. Five-week-old *N. benthamiana* leaves were inoculated with *Agrobacterium* carrying the indicated constructs and incubated for 48 h. Luciferase activity was measured from protein extracts of the leaf samples. Error bars represent SD (n = 3). Letters indicate statistically significant differences (one-way ANOVA, $p < 0.05$). –, inoculation with *Agrobacterium* carrying the empty vector.

(D) ChIP-qPCR analyses of MED25-GFP binding to the G-box from *pJRG21*, *pJAZ6*, and *pJAZ8*. Two-week-old seedlings of *35S:MED25-GFP*/Col-0 plants were pretreated with water (mock) or 0.5 mM SA for 12 h, followed by treatment with water, 50 μM MeJA, or 0.5 mM SA and 50 μM MeJA for 20 min. Error bars represent SD (n = 3). Letters indicate statistically significant differences (two-way ANOVA, $p < 0.0001$). The experiment was performed twice with similar results.

See also Figure S5.

3). Although the former complex has been shown to initiate SA-responsive gene expression (Jin et al., 2018), we demonstrate here that the latter represses JA-responsive and MYC-dependent transcription (Figure 6C). Although some JA-responsive promoters contained TGACG and G-box motifs, NPR1 predominantly localized to the latter motif (Figure 3E; Figure S3A).

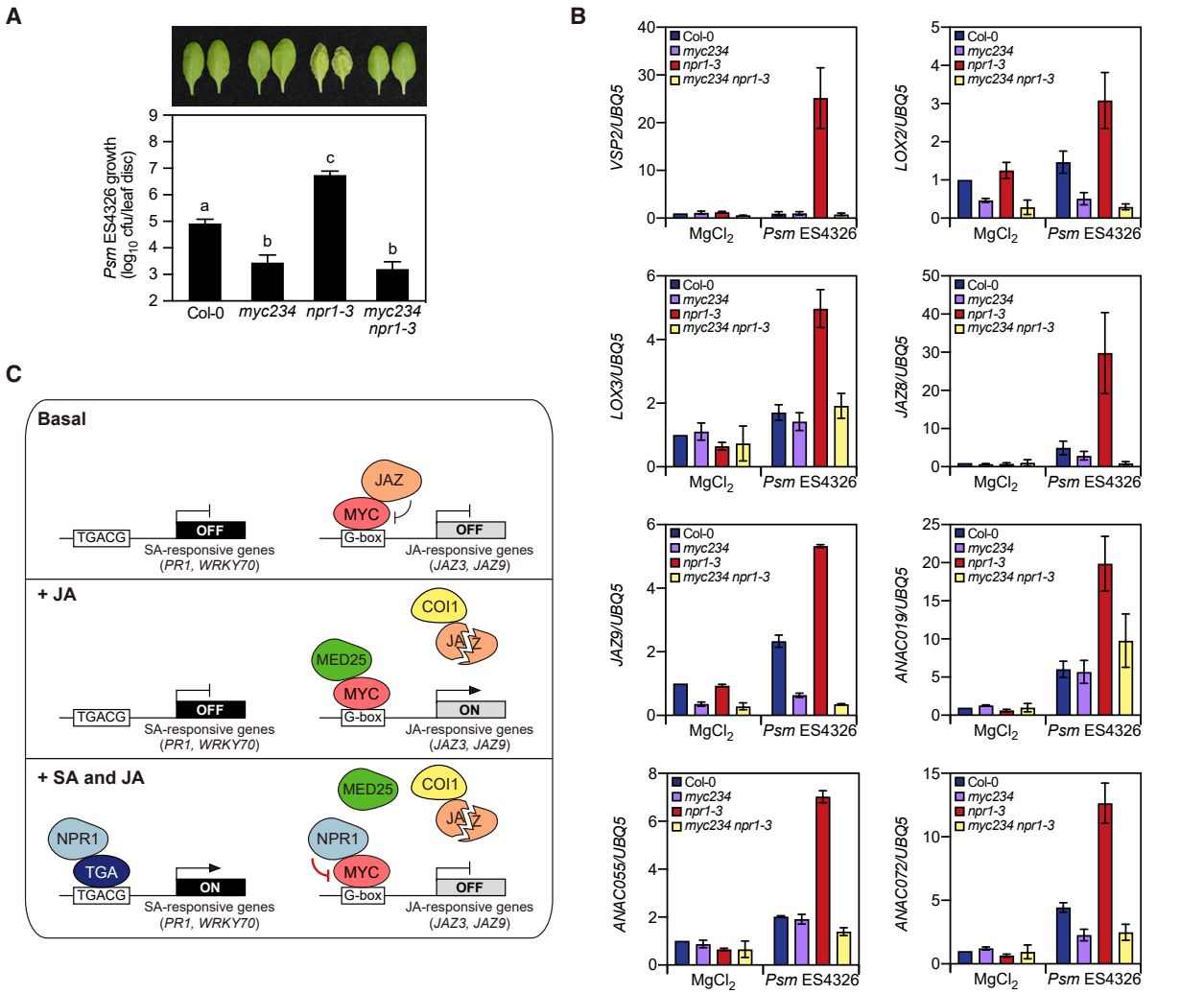

Figure 6. NPR1 suppresses the MYC activator-mediated susceptibility of virulent *Pseudomonas syringae*

(A) Growth of *Psm* ES4326 in the indicated genotypes was monitored 3 days after inoculation (optical density 600 [OD_{600}] = 0.001). Error bars represent SE (n = 7). CFU, colony-forming unit. Letters indicate statistically significant differences (one-way ANOVA, $p < 0.05$).

(B) Four-week-old leaves were inoculated with 10 mM $MgCl_2$ or *Psm* ES4326 (OD_{600} = 0.001) for 24 h. Expression of *VSP2*, *LOX2*, *LOX3*, *JAZ8*, *JAZ9*, *ANAC019*, *ANAC055*, and *ANAC072* was analyzed by qPCR and normalized with *UBQ5*. Error bars represent SD (n = 3).

(C) Proposed model of NPR1-mediated SA/JA crosstalk.

See also Figure S6.

Therefore it is unlikely that TGA factors are responsible for recruitment of NPR1 to JA-responsive genes. We reveal that NPR1 targets the same N-terminal region of MYC2 as JAZ repressors and the MED25 Mediator subunit (Figure 2B), indicating that direct association with MYC2 negates its transcriptional activator activity, possibly by competing for interaction with MED25 (Figure 5C). This notion is supported by our finding that NPR1 occupies many of the same MYC2-regulated promoters as MED25, including JA-responsive *LOX* and *JAZ* genes (Figure 3E; Figure S3A; Spoel et al., 2003; Van der Does et al., 2013; Wang et al., 2019), and that SA treatment reduces JA-induced binding of MED25 to MYC2-targeted promoters to repress their transcriptional activation (Figure 5D). It has been demonstrated that JA facilitates binding of MED25 to the promoter regions of MYC2-targeted genes (Chen et al., 2012), followed by recruitment of histone acetyltransferase 1 (HAC1) and the RNA polymerase II general transcription machinery to initiate MYC2-dependent transcription (An et al., 2017; Zhai et al., 2020). Interestingly, the JA-inducible bHLH proteins MYC2-TARGETED BHLH1 (MTB1), MTB2, and MTB3 have been shown to impair formation of the MED25-MYC2 complex and compete for binding to MYC2-targeted promoters, terminating JA-responsive gene expression (Liu et al., 2019). These results strongly support our hypothesis that NPR1-induced dissociation of the MED25-MYC2 interaction plays a pivotal role in repressing JA-responsive gene expression (Figure 6C). We conclude that SA compromises JA signaling through NPR1-mediated inactivation of MYC activators on JA-responsive promoters.

It has been reported previously that NPR1 may also suppress JA signaling from the cytoplasm rather than the nucleus, as we show here (Spoel et al., 2003). Despite best efforts in that study, it is difficult to exclude all NPR1 from the nucleus, so it remains plausible that a small amount of nuclear NPR1 is sufficient to suppress JA-responsive genes. Alternatively, NPR1 may suppress JA signaling though activities in the cytoplasm and the nucleus. Although cytoplasmic NPR1 may suppress JA signaling in cooperation with other cytosolic proteins, such as MPK4 and PAD4 (Pieterse et al., 2009), nuclear NPR1 suppresses JA-responsive MYC2, as shown in the current study. Although SA and NPR1 likely suppress JA-responsive gene expression via various different mechanisms (Ndamukong et al., 2007; Spoel et al., 2003; Van der Does et al., 2013), our comprehensive genetic and genomic analyses indicate that NPR1-mediated suppression of MYC activity is most predominant and responsible for suppressing pathogen virulence.

The phytotoxin COR is a major virulence factor secreted by a variety of *P. syringae* strains that exerts diverse antagonistic effects on plant immune responses. Because COR is the molecular mimic of an active form of JA, the isoleucine conjugate of JA (JA-Ile), it induces degradation of JAZ proteins to initiate MYC-dependent transcription (Howe et al., 2018; Major et al., 2017). COR has been shown previously to activate three homologous NAC transcription factors, *ANAC019*, *ANAC055*, and *ANAC072*, via MYC2 activity, suppressing SA accumulation and stomatal closure to facilitate pathogen entry into host tissues (Zheng et al., 2012). These structural and functional resemblances to JA-Ile enable antagonistic suppression of SA-induced immune responses through activation of the JA signaling pathway (Brooks et al., 2005; Geng et al., 2014). Our genetic data demonstrate that the enhanced disease susceptibility of *npr1* mutants to COR-producing *Psm* ES4326 is largely recovered by introducing mutations in MYC activators (Figure 6A) and that expression of the above three COR-responsive *NAC*s is repressed in an NPR1-dependent manner (Figure 6B). These data are consistent with the notion that NPR1 counteracts the virulence-promoting activity of COR by abrogating the MYC-dependent signaling pathway.

Functional shifts from coactivator to corepressor behavior, as described here for NPR1, may be a common mechanism utilized by multiple plant transcription cofactors. For example, the lipase-like protein enhanced disease susceptibility 1 (EDS1) positively mediates profound transcriptional changes and host cell death upon recognition of pathogen-secreted effectors by intracellular nucleotide-binding domain/leucine-rich repeat (NLR) receptors (Bhattacharjee et al., 2011; Heidrich et al., 2011). However, EDS1 and its partner PAD4 are also capable of sequestering MYC2 away from the promoter of *ANAC019* to minimize the effect of COR on SA-mediated immune responses (Cui et al., 2018). Another example is that genes responsive to the developmental hormone gibberellin (GA) require DELLA cofactors for appropriate regulation. As corepressors, DELLAs interact with phytochrome-interacting factors (PIFs) to hinder their DNA binding and prevent target gene expression, inhibiting hypocotyl growth (de Lucas et al., 2008; Feng et al., 2008). By contrast, indeterminate domain (IDD) transcription factors that promote expression of the GA regulator *SCARECROW-LIKE 3* (*SCL3*) are activated by interaction with DELLAs (Yoshida et al., 2014). Our findings reveal that the NPR1 cofactor is at the heart of reciprocal regulation of SA- and JA-induced transcriptional programs and ensures appropriate tailoring of immune responses specifically to the attacker. The unexpected mechanistically distinct behaviors of a cofactor in different pathways as a function of transcriptional context may be an important additional mechanism utilized by eukaryotes in general to orchestrate gene expression programs.

Limitations of the study

We demonstrated that SA suppresses the transcriptional activity of MYC activators, which play a major role in the JA signaling pathway. Although SA-mediated repression of the JA signaling pathway includes NPR1-dependent and -independent mechanisms, as shown in our comparative transcriptome analysis, the present model is limited to the mechanism by which NPR1 directly inhibits MYC activators. In addition, there are many JA-responsive genes that are not repressed by SA and/or NPR1. Future study is needed to address the biological role of these genes and the regulatory mechanism of transcription.

Although we showed that NPR1 localizes on JA-responsive promoters via MYC2, we do not exclude the possibility that NPR1 represses a portion of JA-responsive genes by binding to other transcription factors.

The present study demonstrated that the NPR1-MYC2 interaction has a repressive effect on JA-responsive genes but that NPR1-TGA promotes SA-responsive transcription. These different behaviors of NPR1 dependent on transcriptional context should be studied further in the future.

STAR★METHODS

Detailed methods are provided in the online version of this paper and include the following:

- KEY RESOURCES TABLE
- RESOURCE AVAILABILITY
  - Lead contact
  - Materials availability
  - Data and code availability
- EXPERIMENTAL MODEL AND SUBJECT DETAILS
  - Arabidopsis thaliana
  - Nicotiana benthamiana
- METHOD DETAILS
  - Pathogen Infection and Chemical Treatment
  - RNA Analysis
  - Construction of Illumina Sequencing Libraries and Sequencing of RNA
  - Determination of Cis-Regulatory Elements Using RNA-seq Profile
  - Cloning Genes
  - Synthesis of Recombinant Proteins
  - BiFC Assay in *Arabidopsis* Protoplast Cells
  - BiFC Assay in N. benthamiana Leaves
  - *In Vitro* Interaction Assay by AlphaScreen System
  - *In Vitro* Pull-Down Analysis
  - MYC2 and NPR1 Co-immunoprecipitation

SUPPLEMENTAL INFORMATION

Supplemental information can be found online at https://doi.org/10.1016/j.celrep.2021.110125.

ACKNOWLEDGMENTS

We thank X. Dong for *npr1-3* and *35S:NPR1-GFP/npr1-1* plants; R. Solano for *myc2/jin1-2* and *myc234* plants; X. Hou for *pMYC2:MYC2-FLAG/jin1-8*; Q. Xhai for *35S:MED25-GFP*/Col-0; T. Nakagawa for Gateway cloning vectors; K. Ichimura for pSITE vectors; H. Yoshioka for the p19 construct; S. Matsunaga for the histone H2B-tdTomato vector; and K. Murase, J. Fukazawa, W. Inoue, M. Matsumura, K. Miura, K. Okada, N. Oka, and A. Mine for discussion of the work. This work was supported by Grants-in-Aid for Scientific Research on Innovative Areas (JP23120520 and JP25120718) from the Ministry of Education, Culture, Sports, Science and Technology (MEXT, Japan); JSPS KAKENHI (JP15H05956, JP16H05065, and JP20H05906); Cooperative Research Grant 1808 of the Plant Transgenic Design Initiative (PTraD) by the Gene Research Center, Tsukuba-Plant Innovation Research Center, University of Tsukuba, Japan (to Y.T.); a European Research Council (ERC) grant under the European Union Horizon 2020 Research and Innovation Program (grant agreement 678511); the Biotechnology and Biological Sciences Research Council (BB/L006219/1 and BB/S016767/1); a Royal Society University Research Fellowship (UF090321); a Royal Society International Exchanges grant (2014/R2) (to S.H.S.); JSPS KAKENHI (JP13J10800, JP18H06068, and JP19K16165); the Program for Leading Graduate Schools" Integrative Graduate Education and Research in Green Natural Sciences", MEXT, Japan; Cooperative Research Grant 1906/2008/2105 of the PTraD by the Gene Research Center, Tsukuba-Plant Innovation Research Center, University of Tsukuba (to M.N.); and the Japan Science and Technology Agency (ERATO project to T.H.).

AUTHOR CONTRIBUTIONS

Y.T., S.H.S., and M.N. designed the experiments. M.N. performed most of the experiments. M.N. and M.J.S. performed ChIP-qPCR and ChIP-seq analyses. M.J.S. performed co-immunoprecipitation analysis. T.S. and T.H. performed sequencing. M.N., M.T., T.M., and Y.Y.Y. performed promoter analyses. M.N. and H.T. performed the BiFC assay in *Arabidopsis* protoplasts. M.N. and T.I. carried out BiFC and transient assays in *N. benthamiana*. T.S., K.K., and H.M. provided helpful comments and reagents. All authors contributed to manuscript preparation. Y.T., S.H.S., M.N., and M.J.S. wrote the manuscript.

DECLARATION OF INTERESTS

The authors declare no competing interests.

Received: October 14, 2020
Revised: October 5, 2021
Accepted: November 23, 2021
Published: December 14, 2021

SUPPORTING CITATIONS

The following references appear in the Supplemental information: Jiang et al. (2013); Kesarwani et al. (2007); Kleinboelting et al. (2012); Pandey et al. (2010).

REFERENCES

Adachi, H., Nakano, T., Miyagawa, N., Ishihama, N., Yoshioka, M., Katou, Y., Yaeno, T., Shirasu, K., and Yoshioka, H. (2015). WRKY Transcription Factors Phosphorylated by MAPK Regulate a Plant Immune NADPH Oxidase in Nicotiana benthamiana. Plant Cell *27*, 2645–2663.

An, C., Li, L., Zhai, Q., You, Y., Deng, L., Wu, F., Chen, R., Jiang, H., Wang, H., Chen, Q., and Li, C. (2017). Mediator subunit MED25 links the jasmonate receptor to transcriptionally active chromatin. Proc. Natl. Acad. Sci. USA *114*, E8930–E8939.

Bender, C.L., Alarcón-Chaidez, F., and Gross, D.C. (1999). Pseudomonas syringae phytotoxins: mode of action, regulation, and biosynthesis by peptide and polyketide synthetases. Microbiol. Mol. Biol. Rev. *63*, 266–292.

Bhattacharjee, S., Halane, M.K., Kim, S.H., and Gassmann, W. (2011). Pathogen effectors target Arabidopsis EDS1 and alter its interactions with immune regulators. Science *334*, 1405–1408.

Brooks, D.M., Bender, C.L., and Kunkel, B.N. (2005). The Pseudomonas syringae phytotoxin coronatine promotes virulence by overcoming salicylic acid-dependent defences in Arabidopsis thaliana. Mol. Plant Pathol. *6*, 629–639.

Caarls, L., Pieterse, C.M., and Van Wees, S.C. (2015). How salicylic acid takes transcriptional control over jasmonic acid signaling. Front. Plant Sci. *6*, 170.

Cao, H., Bowling, S.A., Gordon, A.S., and Dong, X. (1994). Characterization of an Arabidopsis Mutant That Is Nonresponsive to Inducers of Systemic Acquired Resistance. Plant Cell *6*, 1583–1592.

Cao, H., Glazebrook, J., Clarke, J.D., Volko, S., and Dong, X. (1997). The Arabidopsis NPR1 gene that controls systemic acquired resistance encodes a novel protein containing ankyrin repeats. Cell *88*, 57–63.

Chen, R., Jiang, H., Li, L., Zhai, Q., Qi, L., Zhou, W., Liu, X., Li, H., Zheng, W., Sun, J., and Li, C. (2012). The Arabidopsis mediator subunit MED25 differentially regulates jasmonate and abscisic acid signaling through interacting with the MYC2 and ABI5 transcription factors. Plant Cell *24*, 2898–2916.

Chini, A., Fonseca, S., Fernández, G., Adie, B., Chico, J.M., Lorenzo, O., García-Casado, G., López-Vidriero, I., Lozano, F.M., Ponce, M.R., et al. (2007). The JAZ family of repressors is the missing link in jasmonate signalling. Nature *448*, 666–671.

Crooks, G.E., Hon, G., Chandonia, J.M., and Brenner, S.E. (2004). WebLogo: a sequence logo generator. Genome Res. *14*, 1188–1190.

Cui, H., Qiu, J., Zhou, Y., Bhandari, D.D., Zhao, C., Bautor, J., and Parker, J.E. (2018). Antagonism of Transcription Factor MYC2 by EDS1/PAD4 Complexes Bolsters Salicylic Acid Defense in Arabidopsis Effector-Triggered Immunity. Mol. Plant *11*, 1053–1066.

Dangl, J.L., and Jones, J.D. (2001). Plant pathogens and integrated defence responses to infection. Nature *411*, 826–833.

de Lucas, M., Davière, J.-M., Rodríguez-Falcón, M., Pontin, M., Iglesias-Pedraz, J.M., Lorrain, S., Fankhauser, C., Blázquez, M.A., Titarenko, E., and Prat, S. (2008). A molecular framework for light and gibberellin control of cell elongation. Nature *451*, 480–484.

Després, C., DeLong, C., Glaze, S., Liu, E., and Fobert, P.R. (2000). The Arabidopsis NPR1/NIM1 protein enhances the DNA binding activity of a subgroup of the TGA family of bZIP transcription factors. Plant Cell *12*, 279–290.

Devoto, A., Nieto-Rostro, M., Xie, D., Ellis, C., Harmston, R., Patrick, E., Davis, J., Sherratt, L., Coleman, M., and Turner, J.G. (2002). COI1 links jasmonate signalling and fertility to the SCF ubiquitin-ligase complex in Arabidopsis. Plant J. *32*, 457–466.

Dodds, P.N., and Rathjen, J.P. (2010). Plant immunity: towards an integrated view of plant-pathogen interactions. Nat. Rev. Genet. *11*, 539–548.

Du, M., Zhao, J., Tzeng, D.T.W., Liu, Y., Deng, L., Yang, T., Zhai, Q., Wu, F., Huang, Z., Zhou, M., et al. (2017). MYC2 Orchestrates a Hierarchical Transcriptional Cascade That Regulates Jasmonate-Mediated Plant Immunity in Tomato. Plant Cell *29*, 1883–1906.

Fan, W., and Dong, X. (2002). In vivo interaction between NPR1 and transcription factor TGA2 leads to salicylic acid-mediated gene activation in Arabidopsis. Plant Cell *14*, 1377–1389.

Feng, S., Martinez, C., Gusmaroli, G., Wang, Y., Zhou, J., Wang, F., Chen, L., Yu, L., Iglesias-Pedraz, J.M., Kircher, S., et al. (2008). Coordinated regulation of Arabidopsis thaliana development by light and gibberellins. Nature *451*, 475–479.

Fernández-Calvo, P., Chini, A., Fernández-Barbero, G., Chico, J.M., Gimenez-Ibanez, S., Geerinck, J., Eeckhout, D., Schweizer, F., Godoy, M., Franco-Zorrilla, J.M., et al. (2011). The Arabidopsis bHLH transcription factors MYC3 and MYC4 are targets of JAZ repressors and act additively with MYC2 in the activation of jasmonate responses. Plant Cell *23*, 701–715.

Fu, Z.Q., and Dong, X. (2013). Systemic acquired resistance: turning local infection into global defense. Annu. Rev. Plant Biol. *64*, 839–863.

Fu, Z.Q., Yan, S., Saleh, A., Wang, W., Ruble, J., Oka, N., Mohan, R., Spoel, S.H., Tada, Y., Zheng, N., and Dong, X. (2012). NPR3 and NPR4 are receptors for the immune signal salicylic acid in plants. Nature *486*, 228–232.

Geng, X., Jin, L., Shimada, M., Kim, M.G., and Mackey, D. (2014). The phytotoxin coronatine is a multifunctional component of the virulence armament of Pseudomonas syringae. Planta *240*, 1149–1165.

Hartmann, M., Zeier, T., Bernsdorff, F., Reichel-Deland, V., Kim, D., Hohmann, M., Scholten, N., Schuck, S., Bräutigam, A., Hölzel, T., et al. (2018). Flavin Monooxygenase-Generated N-Hydroxypipecolic Acid Is a Critical Element of Plant Systemic Immunity. Cell *173*, 456–469.e16.

Heidrich, K., Wirthmueller, L., Tasset, C., Pouzet, C., Deslandes, L., and Parker, J.E. (2011). Arabidopsis EDS1 connects pathogen effector recognition to cell compartment-specific immune responses. Science *334*, 1401–1404.

Hino, T., Tanaka, Y., Kawamukai, M., Nishimura, K., Mano, S., and Nakagawa, T. (2011). Two Sec13p homologs, AtSec13A and AtSec13B, redundantly contribute to the formation of COPII transport vesicles in Arabidopsis thaliana. Biosci. Biotechnol. Biochem. *75*, 1848–1852.

Hou, X., Lee, L.Y., Xia, K., Yan, Y., and Yu, H. (2010). DELLAs modulate jasmonate signaling via competitive binding to JAZs. Dev. Cell *19*, 884–894.

Howe, G.A., and Jander, G. (2008). Plant immunity to insect herbivores. Annu. Rev. Plant Biol. *59*, 41–66.

Howe, G.A., Major, I.T., and Koo, A.J. (2018). Modularity in Jasmonate Signaling for Multistress Resilience. Annu. Rev. Plant Biol. *69*, 387–415.

Jiang, S., Yao, J., Ma, K.W., Zhou, H., Song, J., He, S.Y., and Ma, W. (2013). Bacterial effector activates jasmonate signaling by directly targeting JAZ transcriptional repressors. PLoS Pathog. *9*, e1003715.

Jin, H., Choi, S.M., Kang, M.J., Yun, S.H., Kwon, D.J., Noh, Y.S., and Noh, B. (2018). Salicylic acid-induced transcriptional reprogramming by the HAC-NPR1-TGA histone acetyltransferase complex in Arabidopsis. Nucleic Acids Res. *46*, 11712–11725.

Jones, J.D., and Dangl, J.L. (2006). The plant immune system. Nature *444*, 323–329.

Jung, H.W., Tschaplinski, T.J., Wang, L., Glazebrook, J., and Greenberg, J.T. (2009). Priming in systemic plant immunity. Science *324*, 89–91.

Katsir, L., Schilmiller, A.L., Staswick, P.E., He, S.Y., and Howe, G.A. (2008). COI1 is a critical component of a receptor for jasmonate and the bacterial virulence factor coronatine. Proc. Natl. Acad. Sci. USA *105*, 7100–7105.

Kazan, K., and Manners, J.M. (2013). MYC2: the master in action. Mol. Plant *6*, 686–703.

Kesarwani, M., Yoo, J., and Dong, X. (2007). Genetic interactions of TGA transcription factors in the regulation of pathogenesis-related genes and disease resistance in Arabidopsis. Plant Physiol. *144*, 336–346.

Kinkema, M., Fan, W., and Dong, X. (2000). Nuclear localization of NPR1 is required for activation of PR gene expression. Plant Cell *12*, 2339–2350.

Kleinboelting, N., Huep, G., Kloetgen, A., Viehoever, P., and Weisshaar, B. (2012). GABI-Kat SimpleSearch: new features of the Arabidopsis thaliana T-DNA mutant database. Nucleic Acids Res. *40*, D1211–D1215.

Langmead, B., and Salzberg, S.L. (2012). Fast gapped-read alignment with Bowtie 2. Nat. Methods *9*, 357–359.

Li, H., Handsaker, B., Wysoker, A., Fennell, T., Ruan, J., Homer, N., Marth, G., Abecasis, G., and Durbin, R.; 1000 Genome Project Data Processing Subgroup (2009). The Sequence Alignment/Map format and SAMtools. Bioinformatics *25*, 2078–2079.

Liu, Y., Du, M., Deng, L., Shen, J., Fang, M., Chen, Q., Lu, Y., Wang, Q., Li, C., and Zhai, Q. (2019). MYC2 Regulates the Termination of Jasmonate Signaling via an Autoregulatory Negative Feedback Loop. Plant Cell *31*, 106–127.

Ma, W., Noble, W.S., and Bailey, T.L. (2014). Motif-based analysis of large nucleotide data sets using MEME-ChIP. Nat. Protoc. *9*, 1428–1450.

Machanick, P., and Bailey, T.L. (2011). MEME-ChIP: motif analysis of large DNA datasets. Bioinformatics *27*, 1696–1697.

Major, I.T., Yoshida, Y., Campos, M.L., Kapali, G., Xin, X.F., Sugimoto, K., de Oliveira Ferreira, D., He, S.Y., and Howe, G.A. (2017). Regulation of growth-defense balance by the JASMONATE ZIM-DOMAIN (JAZ)-MYC transcriptional module. New Phytol. *215*, 1533–1547.

Maldonado, A.M., Doerner, P., Dixon, R.A., Lamb, C.J., and Cameron, R.K. (2002). A putative lipid transfer protein involved in systemic resistance signalling in Arabidopsis. Nature *419*, 399–403.

Manohar, M., Tian, M., Moreau, M., Park, S.W., Choi, H.W., Fei, Z., Friso, G., Asif, M., Manosalva, P., von Dahl, C.C., et al. (2015). Identification of multiple salicylic acid-binding proteins using two high throughput screens. Front. Plant Sci. *5*, 777.

Martin, K., Kopperud, K., Chakrabarty, R., Banerjee, R., Brooks, R., and Goodin, M.M. (2009). Transient expression in Nicotiana benthamiana fluorescent marker lines provides enhanced definition of protein localization, movement and interactions in planta. Plant J. *59*, 150–162.

Matsushita, T. (2011). A versatile method to prevent transcriptional gene silencing in Arabidopsis thaliana. Plant Biotechnol. *28*, 515–519.

Mi, H., Muruganujan, A., Ebert, D., Huang, X., and Thomas, P.D. (2019). PANTHER version 14: more genomes, a new PANTHER GO-slim and improvements in enrichment analysis tools. Nucleic Acids Res. *47* (*D1*), D419–D426.

Nakamura, S., Mano, S., Tanaka, Y., Ohnishi, M., Nakamori, C., Araki, M., Niwa, T., Nishimura, M., Kaminaka, H., Nakagawa, T., et al. (2010). Gateway binary vectors with the bialaphos resistance gene, bar, as a selection marker for plant transformation. Biosci. Biotechnol. Biochem. *74*, 1315–1319.

Ndamukong, I., Abdallat, A.A., Thurow, C., Fode, B., Zander, M., Weigel, R., and Gatz, C. (2007). SA-inducible Arabidopsis glutaredoxin interacts with TGA factors and suppresses JA-responsive PDF1.2 transcription. Plant J. *50*, 128–139.

Nimchuk, Z., Marois, E., Kjemtrup, S., Leister, R.T., Katagiri, F., and Dangl, J.L. (2000). Eukaryotic fatty acylation drives plasma membrane targeting and enhances function of several type III effector proteins from Pseudomonas syringae. Cell *101*, 353–363.

Nomoto, M., and Tada, Y. (2018). Cloning-free template DNA preparation for cell-free protein synthesis via two-step PCR using versatile primer designs with short 3′-UTR. Genes Cells *23*, 46–53.

O'Connor, T.R., Dyreson, C., and Wyrick, J.J. (2005). Athena: a resource for rapid visualization and systematic analysis of Arabidopsis promoter sequences. Bioinformatics *21*, 4411–4413.

Pandey, S.P., Roccaro, M., Schön, M., Logemann, E., and Somssich, I.E. (2010). Transcriptional reprogramming regulated by WRKY18 and WRKY40 facilitates powdery mildew infection of Arabidopsis. Plant J. *64*, 912–923.

Park, S.W., Kaimoyo, E., Kumar, D., Mosher, S., and Klessig, D.F. (2007). Methyl salicylate is a critical mobile signal for plant systemic acquired resistance. Science *318*, 113–116.

Petrella, R., Caselli, F., Roig-Villanova, I., Vignati, V., Chiara, M., Ezquer, I., Tadini, L., Kater, M.M., and Gregis, V. (2020). BPC transcription factors and a Polycomb Group protein confine the expression of the ovule identity gene SEEDSTICK in Arabidopsis. Plant J. *102*, 582–599.

Pieterse, C.M., Leon-Reyes, A., Van der Ent, S., and Van Wees, S.C. (2009). Networking by small-molecule hormones in plant immunity. Nat. Chem. Biol. *5*, 308–316.

Quinlan, A.R., and Hall, I.M. (2010). BEDTools: a flexible suite of utilities for comparing genomic features. Bioinformatics *26*, 841–842.

Ramírez, F., Ryan, D.P., Grüning, B., Bhardwaj, V., Kilpert, F., Richter, A.S., Heyne, S., Dündar, F., and Manke, T. (2016). deepTools2: a next generation web server for deep-sequencing data analysis. Nucleic Acids Res. *44* (*W1*), W160-5.

R Core Team (2019). R: A language and environment for statistical computing. R Foundation for Statistical Computing, Vienna, Austria.

Robinson, M.D., McCarthy, D.J., and Smyth, G.K. (2010). edgeR: a Bioconductor package for differential expression analysis of digital gene expression data. Bioinformatics *26*, 139–140.

Saleh, A., Withers, J., Mohan, R., Marqués, J., Gu, Y., Yan, S., Zavaliev, R., Nomoto, M., Tada, Y., and Dong, X. (2015). Posttranslational Modifications of the Master Transcriptional Regulator NPR1 Enable Dynamic but Tight Control of Plant Immune Responses. Cell Host Microbe *18*, 169–182.

Sheard, L.B., Tan, X., Mao, H., Withers, J., Ben-Nissan, G., Hinds, T.R., Kobayashi, Y., Hsu, F.F., Sharon, M., Browse, J., et al. (2010). Jasmonate perception by inositol-phosphate-potentiated COI1-JAZ co-receptor. Nature *468*, 400–405.

Skelly, M.J., Furniss, J.J., Grey, H., Wong, K.-W., and Spoel, S.H. (2019). Dynamic ubiquitination determines transcriptional activity of the plant immune coactivator NPR1. eLife *8*, e47005.

Spoel, S.H., and Dong, X. (2012). How do plants achieve immunity? Defence without specialized immune cells. Nat. Rev. Immunol. *12*, 89–100.

Spoel, S.H., Koornneef, A., Claessens, S.M.C., Korzelius, J.P., Van Pelt, J.A., Mueller, M.J., Buchala, A.J., Métraux, J.P., Brown, R., Kazan, K., et al. (2003). NPR1 modulates cross-talk between salicylate- and jasmonate-dependent defense pathways through a novel function in the cytosol. Plant Cell *15*, 760–770.

Spoel, S.H., Johnson, J.S., and Dong, X. (2007). Regulation of tradeoffs between plant defenses against pathogens with different lifestyles. Proc. Natl. Acad. Sci. USA *104*, 18842–18847.

Spoel, S.H., Mou, Z., Tada, Y., Spivey, N.W., Genschik, P., and Dong, X. (2009). Proteasome-mediated turnover of the transcription coactivator NPR1 plays dual roles in regulating plant immunity. Cell *137*, 860–872.

Tada, Y., Spoel, S.H., Pajerowska-Mukhtar, K., Mou, Z., Song, J., Wang, C., Zuo, J., and Dong, X. (2008). Plant immunity requires conformational changes [corrected] of NPR1 via S-nitrosylation and thioredoxins. Science *321*, 952–956.

Thines, B., Katsir, L., Melotto, M., Niu, Y., Mandaokar, A., Liu, G., Nomura, K., He, S.Y., Howe, G.A., and Browse, J. (2007). JAZ repressor proteins are targets of the SCF(COI1) complex during jasmonate signalling. Nature *448*, 661–665.

Thorvaldsdóttir, H., Robinson, J.T., and Mesirov, J.P. (2013). Integrative Genomics Viewer (IGV): high-performance genomics data visualization and exploration. Brief. Bioinform. *14*, 178–192.

Tsukagoshi, H., Saijo, T., Shibata, D., Morikami, A., and Nakamura, K. (2005). Analysis of a sugar response mutant of Arabidopsis identified a novel B3 domain protein that functions as an active transcriptional repressor. Plant Physiol. *138*, 675–685.

Van der Does, D., Leon-Reyes, A., Koornneef, A., Van Verk, M.C., Rodenburg, N., Pauwels, L., Goossens, A., Körbes, A.P., Memelink, J., Ritsema, T., et al. (2013). Salicylic acid suppresses jasmonic acid signaling downstream of SCFCOI1-JAZ by targeting GCC promoter motifs via transcription factor ORA59. Plant Cell *25*, 744–761.

Wang, D., Amornsiripanitch, N., and Dong, X. (2006). A genomic approach to identify regulatory nodes in the transcriptional network of systemic acquired resistance in plants. PLoS Pathog. *2*, e123.

Wang, H., Li, S., Li, Y., Xu, Y., Wang, Y., Zhang, R., Sun, W., Chen, Q., Wang, X.J., Li, C., and Zhao, J. (2019). MED25 connects enhancer-promoter looping and MYC2-dependent activation of jasmonate signalling. Nat. Plants *5*, 616–625.

Wu, Y., Zhang, D., Chu, J.Y., Boyle, P., Wang, Y., Brindle, I.D., De Luca, V., and Després, C. (2012). The *Arabidopsis* NPR1 protein is a receptor for the plant defense hormone salicylic acid. Cell Rep. *1*, 639–647.

Xie, D.-X., Feys, B.F., James, S., Nieto-Rostro, M., and Turner, J.G. (1998). COI1: an Arabidopsis gene required for jasmonate-regulated defense and fertility. Science *280*, 1091–1094.

Xu, L., Liu, F., Lechner, E., Genschik, P., Crosby, W.L., Ma, H., Peng, W., Huang, D., and Xie, D. (2002). The SCF(COI1) ubiquitin-ligase complexes are required for jasmonate response in Arabidopsis. Plant Cell *14*, 1919–1935.

Yamaguchi, N., Winter, C.M., Wu, M.F., Kwon, C.S., William, D.A., and Wagner, D. (2014). PROTOCOLS: Chromatin Immunoprecipitation from Arabidopsis Tissues. Arabidopsis Book *12*, e0170.

Yamamoto, Y.Y., Yoshioka, Y., Hyakumachi, M., Maruyama, K., Yamaguchi-Shinozaki, K., Tokizawa, M., and Koyama, H. (2011). Prediction of transcriptional regulatory elements for plant hormone responses based on microarray data. BMC Plant Biol. *11*, 39.

Yan, Y., Stolz, S., Chételat, A., Reymond, P., Pagni, M., Dubugnon, L., and Farmer, E.E. (2007). A downstream mediator in the growth repression limb of the jasmonate pathway. Plant Cell *19*, 2470–2483.

Yoshida, H., Hirano, K., Sato, T., Mitsuda, N., Nomoto, M., Maeo, K., Koketsu, E., Mitani, R., Kawamura, M., Ishiguro, S., et al. (2014). DELLA protein functions as a transcriptional activator through the DNA binding of the indeterminate domain family proteins. Proc. Natl. Acad. Sci. USA *111*, 7861–7866.

Zhai, Q., Deng, L., and Li, C. (2020). Mediator subunit MED25: at the nexus of jasmonate signaling. Curr. Opin. Plant Biol. *57*, 78–86.

Zhang, Y., Liu, T., Meyer, C.A., Eeckhoute, J., Johnson, D.S., Bernstein, B.E., Nusbaum, C., Myers, R.M., Brown, M., Li, W., and Liu, X.S. (2008). Model-based analysis of ChIP-Seq (MACS). Genome Biol. *9*, R137.

Zhang, F., Yao, J., Ke, J., Zhang, L., Lam, V.Q., Xin, X.F., Zhou, X.E., Chen, J., Brunzelle, J., Griffin, P.R., et al. (2015). Structural basis of JAZ repression of MYC transcription factors in jasmonate signalling. Nature *525*, 269–273.

Zheng, X.Y., Spivey, N.W., Zeng, W., Liu, P.P., Fu, Z.Q., Klessig, D.F., He, S.Y., and Dong, X. (2012). Coronatine promotes Pseudomonas syringae virulence in plants by activating a signaling cascade that inhibits salicylic acid accumulation. Cell Host Microbe *11*, 587–596.

STAR★METHODS

KEY RESOURCES TABLE

REAGENT or RESOURCE	SOURCE	IDENTIFIER
Antibodies		
Rabbit polyclonal anti-GFP (ChIP grade)	Abcam	Cat# ab290; RRID:AB_303395
Rabbit IgG, polyclonal-Isotype Control	Abcam	Cat# ab37415; RRID:AB_2631996
Mouse monoclonal anti-FLAG M2 affinity gel	Sigma-Aldrich	Cat# A2220; RRID:AB_10063035
Rabbit polyclonal anti-HA	Santa Cruz Biotechnology	Cat# sc-805; RRID:AB_631618
Mouse monoclonal anti-DYKDDDDK	WAKO	Cat# 014-22383; RRID:AB_10660291
Rabbit polyclonal anti-FLAG	Sigma-Aldrich	Cat# SAB4301135; RRID:AB_2811010
NPR1 antibody	AgriSera	Cat# AS12 1854
Goat anti Rabbit IgG (H+L) antibody, HRP conjugate	Bio-Rad	Cat# 170-6515; RRID:AB_11125142
Goat anti-mouse IgG (H+L) antibody, HRP conjugate	Proteintech	Cat# SA00001-1; RRID:AB_2722565
Pierce High Sensitivity NeutrAvidin-HRP	Thermo Fisher Scientific	Cat# 31030
Bacterial and virus strains		
Escherichia coli strain JM109	Takara Bio	Cat# 9052
Agrobacterium tumefaciens strain GV3101 (pMP90)	Tada lab stock	N/A
Pseudomonas syringae pv. *maculicola* ES4326	Tada lab stock	N/A
Chemicals, peptides, and recombinant proteins		
Protease Inhibitor Cocktail	Sigma-Aldrich	Cat# P9599
Sodium salicylate (SA)	WAKO	Cat# 195-03145
Methyl-jasmonate (JA)	Sigma-Aldrich	Cat# 392707
Critical commercial assays		
Cell-Free Protein Synthesis Kit	BioSieg	N/A
NEB Ultra II DNA Library Prep Kit for Illumina	New England BioLabs	Cat# E7645S
Dual-Luciferase® Reporter Assay System	Promega	Cat# E1910
TruSeq RNA Sample Preparation kit	Illumina	Cat# FC-122-1001
AlphaScreen FLAG (M2) Detection Kit	PerkinElmer	Cat# 6760613C
Deposited data		
RNA-seq	This paper	DRA003119
ChIP-seq of NPR1	This paper	DRA010718
ChIP-seq of MYC2 and MED25	Wang et al., 2019	CRA001078
Arabidopsis thaliana genome	TAIR10	https://www.arabidopsis.org/
Experimental models: Organisms/strains		
Arabidopsis: 35S:NPR1-GFP/npr1-1	Kinkema et al., 2000	N/A
Arabidopsis: pMYC2:MYC2-FLAG/jin1-8	Hou et al., 2010	N/A
Arabidopsis: 35S:NPR1-GFP/npr1-1 jin1-2	This paper	N/A
Arabidopsis: myc234	Fernández-Calvo et al., 2011	GK445B11, GK491E10
Arabidopsis: myc234 npr1-3	This paper	N/A
Arabidopsis: npr1-3	Cao et al., 1994	N/A
Recombinant DNA		
pDONR221	Invitrogen	Cat# 12536017
pPZP200 (masP)	Matsushita, 2011	N/A

(*Continued on next page*)

Continued

REAGENT or RESOURCE	SOURCE	IDENTIFIER
pGWcY	Hino et al., 2011	N/A
pnYGW	Hino et al., 2011	N/A
pcYGW	Hino et al., 2011	N/A
pGWB635	Nakamura et al., 2010	N/A
pGWB605	Nakamura et al., 2010	N/A
pGWB611	Nakamura et al., 2010	N/A
pSITE-cEYFP-N1	Martin et al., 2009	N/A
pSITE-cEYFP-C1	Martin et al., 2009	N/A
pSITE-nEYFP-C1	Martin et al., 2009	N/A
Software and algorithms		
R (version 4.0.0)	R Core Team, 2019	https://www.r-project.org
Bowtie2 (version 2.3.5.1)	Langmead and Salzberg, 2012	http://bowtie-bio.sourceforge.net/bowtie2/index.shtml
SAMtools (version 1.9)	Li et al., 2009	http://samtools.sourceforge.net/
MACS2 (version 2.0.9)	Zhang et al., 2008	https://taoliu.github.io/MACS/
deepTools (version 2.25.0)	Ramírez et al., 2016	https://deeptools.readthedocs.io/en/develop/
IGV (version 2.5.0)	Thorvaldsdóttir et al., 2013	http://software.broadinstitute.org/software/igv/
Bedtools (version 2.25.0)	Quinlan and Hall, 2010	https://bedtools.readthedocs.io/en/latest/
MEME-ChIP (version 5.1.1)	Machanick and Bailey, 2011	https://meme-suite.org/tools/meme-chip
PANTHER (Released 20200407)	Mi et al., 2019	https://www.arabidopsis.org/tools/go_term_enrichment.jsp

RESOURCE AVAILABILITY

Lead contact

Further information and requests for resources and reagents should be directed to and will be fulfilled by the Lead Contact, Yasuomi Tada (ytada@gene.nagoya-u.ac.jp).

Materials availability

All materials generated in this study are available from the Lead Contact.

Data and code availability

- RNA sequencing and ChIP sequencing data generated in this paper have been deposited in the DDBJ Sequence Read Archive (DRA) at the DNA Data Bank (DDBJ; https://www.ddbj.nig.ac.jp/) and are publicly available as of the data of publication. Accession numbers are listed in the Key resources table.
- This paper does not report original code.
- Any additional information required to reanalyze the data reported in this paper is available from the Lead Contact upon request.

EXPERIMENTAL MODEL AND SUBJECT DETAILS

Arabidopsis thaliana

Arabidopsis (*Arabidopsis thaliana*) transgenic lines and mutants used in this study were derived from Columbia (Col-0) ecotype. For pathogen infection, all plants were grown in soil (Sakata Seed Co. Ltd., Yokohama, Japan) under a 16 h light and 8 h dark cycle at 22°C with 65% relative humidity. For RT-qPCR and ChIP analyses, *Arabidopsis* seedlings were grown on vertical half-strength Murashige and Skoog (MS) plates [1% (w/v) sucrose, 0.6% (w/v) gellan gum, and 0.01% (w/v) myo-inositol, pH 5.7] in a growth chamber (CLE-303, Tomy Kogyo Co. Ltd., Tokyo, Japan) at 22°C under a 16 h light and 8 h dark cycle.

The *35S:NPR1-GFP/npr1-1* transgenic plants were provided by Dr. Xinnian Dong (Duke University, Durham, USA). The *pMYC2:MYC2-FLAG/jin1-8* transgenic plants were provided by Dr. Xingliang Hou (Chinese Academy of Sciences, Beijing, China). The *jin1-2/myc2* and *myc234* mutants were provided by Dr. Roberto Solano (Centro Nacional de Biotecnología-CSIC, Madrid, Spain).

The *35S:MED25-GFP*/Col-0 transgenic plants were provided by Dr. Qingzhe Zhai (Chinese Academy of Sciences, Beijing, China). The *npr1-3* mutant was crossed with *myc234* plants to generate the *myc234 npr1-3* quadruple mutant. The *jin1-2* mutant was crossed with *35S:NPR1-GFP/npr1-1* plants to generate the *35S:NPR1-GFP/npr1-1 jin1-2*. Primers used for genotyping F2 and F3 plants are listed in Table S3.

Nicotiana benthamiana

N. benthamiana (kind gift from Dr. Kazuya Ichimura, Kagawa University) was grown in soil (Sakata Seed Co. Ltd., Yokohama, Japan) under a 16 h light and 8 h dark cycle at 25°C. Five-week-old *N. benthamiana* leaves were used in all experiments in this study.

METHOD DETAILS

Pathogen Infection and Chemical Treatment

Pseudomonas syringae pv. *maculicola* (*Psm*) ES4326 (OD_{600} = 0.001) was pressure infiltrated into whole leaves of 4-week-old plants using a needleless syringe, and bacterial growth was determined 3 days after inoculation as described previously (Wang et al., 2006). For RT-qPCR analysis, whole leaves were infiltrated with *Psm* ES4326 (OD_{600} = 0.001) and collected 24 h after inoculation. The leaf tissue was stored at −80°C until use.

For RT-qPCR analysis, thirteen-day-old seedlings were pretreated with water or 0.5 mM sodium salicylate (SA; Wako Pure Chemical Industries, Ltd., Osaka, Japan) for 12 h, followed by incubation with water, 0.5 mM SA, 50 μM methyl-jasmonate (JA; Sigma-Aldrich, Co., MO, USA), or both SA and JA for 4 h. Three seedlings were mixed and processed for the expression analysis as described in "RNA Analysis." The leaf tissue was stored at −80°C until use.

RNA Analysis

Total RNA was isolated using the RNeasy® Mini Kit (QIAGEN, Hilden, Germany) from seedlings treated with hormones or leaves inoculated with *Psm* ES4326 as described above. First-strand cDNA was synthesized from 500 ng of total RNA using the PrimeScript RT Reagent Kit (Takara Bio, Inc., Shiga, Japan) according to the manufacturer's instructions. Quantitative real-time PCR was carried out on a LightCycler® (Roche, Basel, Switzerland) using the KAPA SYBR® FAST qPCR Master Mix (2x) kit (Kapa Biosystems, Inc., NC, USA), 20-fold diluted cDNAs, and the gene-specific primers listed in Table S3. Each experiment had three biological replicates and was repeated at least three times.

Construction of Illumina Sequencing Libraries and Sequencing of RNA

RNA samples were isolated with the RNeasy® Mini Kit (QIAGEN), and analyzed by qPCR. For RNA-Seq, cDNA libraries were constructed from 1 μg of RNA samples by a TruSeq RNA Sample Preparation kit (Illumina, CA, USA) and the amount of cDNA was determined by Phix control (Illumina). The single end of cDNA libraries was sequenced for 36 nucleotides with an Illumina GAIIx sequencer, reads were mapped to the *Arabidopsis thaliana* genome (TAIR10; https://www.arabidopsis.org/) by Bowtie (Langmead and Salzberg, 2012), and pairwise comparisons were performed with EdgeR (Robinson et al., 2010). Differentially expressed genes were selected with a fold change > 1 and an FDR < 0.01.

Determination of Cis-Regulatory Elements Using RNA-seq Profile

JA-induced genes, which were repressed in an NPR1-dependent manner, were identified by RNA-seq (Table S1; Figures S1A and S1B). Extraction of overrepresented octamer sequences was performed as previously reported (Yamamoto et al., 2011). The enriched octamers were aligned according to a conserved pentamer sequence, followed by the Weblogo analysis using Weblogo version 2.8.2 (http://weblogo.berkeley.edu/) (Crooks et al., 2004). The conserved pentamers were used to demonstrate the motifs in Figures S1C and S1D. Promoter sequences were also subjected to Athena analyses that determine the enriched *cis*-regulatory elements on a gene set (O'Connor et al., 2005).

Cloning Genes

To clone genes of transcription regulators, template cDNAs were prepared from wild-type leaves treated with 0.5 mM SA or 50 μM MeJA as described above. Target genes were amplified using a GeneAtlas (Astec, Fukuoka, Japan) and cloned into pDONR221 (Invitrogen, CA, USA) with the Gateway cloning system (Gateway® BP Clonase Enzyme mix, Invitrogen). The primers used for cloning and verification of DNA sequences are listed in Table S3.

Synthesis of Recombinant Proteins

Protein synthesis was performed using the Cell-Free Protein Synthesis Kit following the manufacturer's instructions (BioSieg, Tokushima, Japan). For *in vitro* transcription, the coding DNA sequences of either FLAG tag (DYKDDDDK) or the biotin acceptor peptide (BAP tag: GLNDIFEAQKIEWHE) were attached to the cDNA templates of transcription factors by PCR using KOD-Plus-Neo DNA polymerase (TOYOBO, Osaka, Japan). Approximately 30 μg of RNA was prepared by T7 RNA polymerase-based transcription from the PCR product (Nomoto and Tada, 2018). The RNA samples were dissolved in 70 μL of RNase-free water (Invitrogen) and mixed with 20 μL of a wheat germ extract and 20 μL of amino acid mixture at 16°C for 10-18 h. Biotinylation of BAP-tagged proteins was

performed during the protein synthesis in the above mixture supplemented with 0.33 μL of biotin ligase BirA and 5 μL of d-Biotin (Avidity, LLC, CO, USA). The biotinylated proteins were then dialyzed against 1 x PBS (137 mM NaCl, 8.1 mM Na_2HPO_4, 2.68 mM KCl, and 1.47 mM KH_2PO_4) at 4°C for 16-22 h. The synthesized proteins were confirmed by immunoblotting with an antibody against FLAG (Wako), an antibody against HA (Santa Cruz Biotechnology, Inc., CA, USA), or neutravidin conjugated to horseradish peroxidase (Thermo Fisher Scientific Inc., IL, USA).

BiFC Assay in *Arabidopsis* Protoplast Cells

Arabidopsis protoplasts were prepared as previously described (Tsukagoshi et al., 2005). The cDNAs of *NPR1*, *JAZ1*, and *MYC2* in pDONR221 were subcloned into the 35S CaMV promoter-driven destination vectors pGWcY, pnYGW, or pcYGW (kind gifts from Dr. Tsuyoshi Nakagawa, Shimane University) (Hino et al., 2011) by LR clonase reaction (Gateway® LR Clonase Enzyme mix, Invitrogen). A 150 μl suspension of 5 × 10^6 cells/ml was transfected with 15 μg of *NPR1* or *JAZ1* cDNAs plus 15 μg of *MYC2* cDNA by 65 μl of 40% (w/v) polyethylene glycol (Polyethylene Glycol 4,000, Wako). After 20 min incubation on ice, samples were mixed with 5 mL of dilution solution (1.5 mM MES-KOH, pH 5.6, 400 mM mannitol, 125 mM $CaCl_2$, 4.98 mM KCl, and 50 mM glucose) and centrifuged at 600 rpm at room temperature for 5 min. The pellets were resuspended in 2 mL of MS-mannitol solution [1 x MS, 400 mM mannitol, pH 5.7, 3.3 mM $CaCl_2$, 0.1% (w/v) myo-inositol, and 0.001% (w/v) thiamine-HCl] and incubated at 22°C for 12 h in the dark. Samples were viewed under a Leica DMI6000 B with a 40X objective lens (Leica Microsystems, Wetzlar, Germany).

BiFC Assay in N. benthamiana Leaves

The cDNAs of *NPR1*, *JAZ1*, *MYC2*, *MYC3*, and *MYC4* in pDONR221 were cloned into the 35S CaMV promoter-driven destination vectors pSITE-cEYFP-N1, pSITE-cEYFP-C1, or pSITE-nEYFP-C1 (kind gifts from Dr. Kazuya Ichimura, Kagawa University) (Martin et al., 2009) by LR clonase reaction (Gateway® LR Clonase Enzyme mix, Invitrogen). These constructs were transformed into *Agrobacterium tumefaciens* strain GV3101 using the freeze-thaw method. The *Agrobacterium* was resuspended in 4 mL of Agrobacterium Induction Media (AIM) with 150 μg/ml Acetosyringone as previously described (Nimchuk et al., 2000). After incubation at 210 rpm at 28°C for 5 h, samples were centrifuged at 4,000 rpm at room temperature for 20 min. The pellets were resuspended in infiltration buffer (0.5 mM MES-KOH, pH 5.6, 1 mM $MgCl_2$, 50 μg/ml Acetosyringone), and each transformed cell and *Agrobacterium* carrying p19 suppressor from *Tomato bushy stunt virus* (Adachi et al., 2015) and histone H2B-tdTomato (kind gift from Dr. Sachihiro Matsunaga, Tokyo University) were mixed in different combinations to a final concentration of OD_{600} = 0.1. Five-week-old *N. benthamiana* leaves were co-infiltrated with the mixed *Agrobacterium* cells, and placed under a 16 h of light and 8 h of dark cycle at 25°C for 60 h. Sample leaves were viewed under a DMI 6000B-AFC fluorescence microscope and a SP8 confocal microscope with a 10X objective lens (Leica Microsystems).

In Vitro Interaction Assay by AlphaScreen System

In vitro protein-protein interactions were evaluated by the AlphaScreen system (PerkinElmer Inc., MA, USA) according to the manufacturer's instructions. Briefly, 2 μl of FLAG-tagged MYC transcription factors (33 ng) and biotinylated NPR1 or JAZ1 (18.5 ng) produced by the *in vitro* translation system were incubated with 2.5 μl of 10 x Control Buffer [FLAG (M2) Detection Kit, PerkinElmer Inc.], 2.5 μl of 0.1% (w/v) Tween® 20, 2.5 μl of 1% (w/v) BSA, and 5.5 μl of ultrapure water at room temperature for 1 h. Samples were mixed with 4 μl of 40-fold diluted Acceptor Bead and then incubated at room temperature for 1 h, followed by the reaction with 4 μl of 40-fold diluted Donor Bead for 6-12 h. Upon excitation at 680 nm, the emission wavelengths between 520 and 620 nm were measured as AlphaScreen units (interaction signals) using a Spark 10M Multimode Microplate Reader (TECAN, Männedorf, Switzerland).

In Vitro Pull-Down Analysis

10 μl of MYC2-FLAG and 30 μl of NPR1-HA *in vitro*-synthesized proteins were incubated with 460 μl of Buffer A [1 x PBS, 0.01% (w/v) Tween® 20, 0.04 mM MG115, and protease inhibitor cocktail (Sigma-Aldrich)] at 16°C for 3 h. For the MYC2-FLAG negative control, the equivalent amount of a wheat germ extract was added to the mixture. Samples were then incubated with 2 μL of an antibody against FLAG (Wako) at 16°C for 1 h with gentle rocking while a 10 μL aliquot was used as the input control, followed by incubation with 25 μl Dynabeads® Protein A bead slurry (Invitrogen) at 16°C for 1 h with gentle rocking. The beads were washed with 1 mL of Buffer B [1 x PBS, 0.01% (w/v) Tween® 20], and incubated in 20 μl of sample buffer [75 mM Tris-HCl, pH 6.8, 15% (w/v) glycerol, 0.03% (w/v) bromophenol blue, 3% (w/v) sodium dodecyl sulfate (SDS), and 200 mM dithiothreitol (DTT)] at 70°C for 20 min. Samples were then subjected to SDS polyacrylamide gel electrophoresis (SDS-PAGE), followed by immunoblotting for FLAG- and HA-tagged proteins.

For the competition assay, 8 μl of 2.8-fold diluted MYC2-HA and 40 μl or 80 μl of 2-fold diluted NPR1-BAP were incubated with Buffer A (total 400 μl) at 4°C for 12 h. For the negative control, the equivalent amount of a wheat germ extract was added to the mixture. Samples were then mixed with 3 μl of 2.8-fold diluted FLAG-JAZ1 and 1 μL of an antibody against FLAG (Wako), and incubated at 4°C for 40 min with gentle rocking while a 10 μL aliquot was used as the input control. Samples were then incubated with 25 μl Dynabeads® Protein A bead slurry (Invitrogen) at 16°C for 45 min. The beads were washed 3 times with 1 mL of Buffer B, and incubated in 30 μl of sample buffer at 70°C for 20 min. Samples were then subjected to SDS-PAGE, followed by immunoblotting for HA, FLAG, and BAP-tagged proteins.

MYC2 and NPR1 Co-immunoprecipitation

For NPR1 co-immunoprecipitation with MYC2-FLAG, 0.5 g of seedlings per sample were pretreated with 0.5 mM SA for 12 h, followed by treatment with water, 0.5 mM SA, 50 μM JA, or both SA and JA for 4 h. Tissue was frozen and ground to a fine powder in liquid nitrogen before homogenizing in protein extraction buffer [50 mM Tris-HCl, pH 7.5, 150 mM NaCl, 5 mM EDTA, 0.1% (w/v) Triton X-100, 0.2% (w/v) Nonidet P-40, and inhibitors: 50 μg/ml TPCK, 50 μg/ml TLCK, 0.6 mM PMSF]. Extracts were centrifuged at 13,000 rpm at 4°C for 20 min to remove cellular debris and filtered through 0.22 μm filters. Anti-FLAG M2 affinity gel (Sigma-Aldrich) was washed with the above buffer before incubating with samples overnight with rotation at 4°C. The resin was washed 5 times with the same buffer before immunoprecipitated proteins were eluted by boiling in 1 x SDS-PAGE sample buffer including 50 mM DTT. MYC2-FLAG was detected using rabbit anti-FLAG antibodies (Sigma-Aldrich) while co-immunoprecipitating NPR1 was detected with anti-NPR1 antibodies (AgriSera, Vännäs, Sweden).

Fluorescence Microscopy of NPR1-GFP Proteins

Thirteen-day-old *35S:NPR1-GFP/npr1-1* seedlings were pretreated with water for 12 h, followed by treatment with water, 0.5 mM SA, 50 μM JA, or both SA and JA for 6 h as described above. Sample leaves were viewed under a fluorescence microscope BZ-X800 with a 40X objective lens (KEYENCE, Osaka, Japan).

ChIP Assay

Approximately 0.7 g of 2-week-old *pMYC2:MYC2-FLAG/jin1-8* seedlings were pretreated with water or SA for 12 h, followed by treatment with water, 0.5 mM SA, 50 μM JA, or both SA and JA for 4 h as described above. Approximately 0.7 g of 2-week-old *35S:MED25-GFP*/Col-0 seedlings were pretreated with water or SA for 12 h, followed by treatment with water, 50 μM JA, or both SA and JA for 20 min. Similarly, approximately 0.7 g of *35S:NPR1-GFP/npr1-1* and *35S:NPR1-GFP/npr1-1 jin1-2* seedlings were subjected to treatment with water, 0.5 mM SA, 50 μM JA, or both SA and JA for 6 h as described above. Samples were fixed in 25 mL of 1% formaldehyde under vacuum for 3 cycles of 2 min ON/2min OFF using an aspirator (SIBATA, Saitama, Japan). Subsequently, 1.5 mL of 2 M glycine was added to quench the cross-linking reaction under vacuum for 2 min. The sample tissues were then washed with 50 mL of double-distilled water and stored at −80°C until use. Frozen samples were ground to a fine powder with a mortar and pestle in liquid nitrogen and dissolved in 2.5 mL of nuclei extraction buffer (10 mM Tris-HCl, pH 8.0, 0.25 M sucrose, 10 mM $MgCl_2$, 40 mM β-mercaptoethanol, and protease inhibitor cocktail) (Yamaguchi et al., 2014). Samples were filtered through two layers of Miracloth (Calbiochem, CA, USA) and centrifuged at 13,500 rpm at 4°C for 5 min. The pellets were resuspended in 75 μL of nuclei lysis buffer [50 mM Tris-HCl, pH 8.0, 10 mM EDTA, 1% (w/v) SDS]. After incubation at room temperature for 20 min then on ice for 10 min, samples were mixed with 225 μL of ChIP dilution buffer without Triton [16.7 mM Tris-HCl, pH 8.0, 167 mM NaCl, 1.2 mM EDTA, and 0.01% (w/v) SDS]. Chromatin samples were sonicated for 10 cycles of 30 s ON/30 s OFF using a Bioruptor UCW-201 (Cosmo Bio Co., Ltd., Tokyo, Japan) to produce DNA fragments, followed by the addition of 375 μL of ChIP dilution buffer without Triton, 200 μL of ChIP dilution buffer with Triton [16.7 mM Tris-HCl, pH 8.0, 167 mM NaCl, 1.2 mM EDTA, 0.01% (w/v) SDS, and 1.1% (w/v) Triton X-100], and 35 μL of 20% (w/v) Triton X-100. After centrifugation at 13,500 rpm at 4°C for 5 min, 900 μL of solubilized sample was transferred to protein low-binding tubes and incubated with 100 μL of anti-FLAG® M2 affinity gel slurry (Sigma-Aldrich) or 0.7 μL of an anti-GFP antibody (Abcam, Cambridge, UK) for 2 h with gentle rocking while an 18 μL aliquot was used as the input control. Then, samples were mixed with 100 μl Protein A agarose bead slurry (Upstate, Darmstadt, Germany) and incubated at 4°C for 1 h with gentle rocking. Beads were washed twice with 1 mL of low salt wash buffer [20 mM Tris-HCl, pH 8.0, 150 mM NaCl, 2 mM EDTA, 0.1% (w/v) SDS, and 1% (w/v) Triton X-100], twice with 1 mL of high salt wash buffer [20 mM Tris-HCl, pH 8.0, 500 mM NaCl, 2 mM EDTA, 0.1% (w/v) SDS, and 1% (w/v) Triton X-100], twice with 1 mL of LiCl wash buffer [10 mM Tris-HCl, pH 8.0, 0.25 M LiCl, 1 mM EDTA, 1% (w/v) sodium deoxycholate, and 1% (w/v) Nonidet P-40], and twice with 1 mL of TE buffer [10 mM Tris-HCl, pH 8.0, 1 mM EDTA]. After washing, beads were resuspended in 100 μL of elution buffer [1% (w/v) SDS, 0.1 M $NaHCO_3$, and 1 μg/ml salmon sperm DNA] and incubated at 65°C for 30 min. For the input controls, 41.14 μL of TE buffer, 8.7 μL of 10% (w/v) SDS, 21 μL of elution buffer, and 1 μg/ml salmon sperm DNA were added to 18 μL of each solubilized sample. Both supernatant and input samples were mixed with 4 μL of 5 M NaCl and incubated at 65°C overnight to reverse crosslinks, followed by digestion with 1 μL of Proteinase K (Invitrogen) at 37°C for 1 h. ChIP samples were mixed with 500 μL of Buffer NTB and purified using the PCR clean-up Gel extraction following the manufacturer's instructions (MACHEREY-NAGEL, Düren, Germany). Quantitative real-time PCR was carried out on a LightCycler® (Roche) using the KAPA SYBR® FAST Universal 2X qPCR Master Mix (Kapa Biosystems, Inc.), 5-fold diluted purified DNAs, and gene-specific primers listed in Table S3.

For ChIP-seq analysis, approximately 0.7 g of *35S:NPR1-GFP/npr1-1* seedlings were subjected to treatment with water or both SA and JA for 6 h as described above. Chromatin samples were sonicated for 30 cycles of 30 s ON/30 s OFF. The sonicated samples were split into 2 tubes, followed by the addition of 560 μL ChIP dilution buffer with Triton and 0.5 μL of an anti-GFP antibody (IP) (Abcam) or Rabbit IgG-Isotype Control (Control) (Abcam). Next, each sample was mixed with 50 μl of Protein A agarose bead slurry (Upstate) and incubated at 4°C for 3 h with gentle rocking. Beads were washed as described above then resuspended in 100 μL of elution buffer [1% (w/v) SDS, 0.1 M $NaHCO_3$] and incubated at 65°C for 30 min. Supernatants were mixed with 4 μL of 5 M NaCl and incubated at 65°C overnight, followed by the digestion with 1 μL of Proteinase K (Invitrogen) at 37°C for 1 h. DNA samples were purified using the PCR clean-up Gel extraction following the manufacturer's instructions (MACHEREY-NAGEL).

Construction of Illumina Sequencing Libraries and Sequencing of ChIP DNA

ChIP-seq libraries for three biological replicates were constructed from 200 ng of DNA samples using the NEB Ultra II DNA Library Prep Kit for Illumina (New England BioLabs, MA, USA) according to the manufacturer's instructions. The amount of cDNA was determined by the QuantiFluor® dsDNA System (Promega, WI, USA). All ChIP-seq libraries were sequenced as 86-bp single-end reads using the Illumina system NextSeq500.

Analysis of ChIP-Seq Data

Reads were mapped to the *Arabidopsis thaliana* genome (TAIR10; https://www.arabidopsis.org/) using Bowtie2 with default parameters (Langmead and Salzberg, 2012). The Sequence Alignment/Map (SAM) file generated by Bowtie2 was converted to a Binary Alignment/Map (BAM) format file by SAMtools (Li et al., 2009). To visualize the mapped reads, the Tiled Data File (TDF) file was generated from the BAM file using the igvtools package in the Integrative Genome Browser (IGV) (Thorvaldsdóttir et al., 2013). The read coverages for three biological replicates were compared with multiBamSummary from deepTools with 100-b bins (Ramírez et al., 2016), and the output was visualized by plotCorrelation. The bamCoverage command was used to generate a coverage track as the BigWig file and plotHeatmap visualized the scores. ChIP-seq peaks were called by comparing the IP with the Input using Model-based Analysis of ChIP-Seq (MACS2) with the "-p 0.05 -g 1.118e8" option ($p < 0.05$ and peak score > 30) (Zhang et al., 2008). The peaks were annotated with the nearest gene using the Bioconductor and ChIPpeakAnno package in R program. Gene Ontology (GO) analysis of the set of 2554 genes detected across three biological replicates was performed by PANTHER (Mi et al., 2019) in The *Arabidopsis* Information Resource (TAIR) website (https://www.arabidopsis.org/tools/go_term_enrichment.jsp). Sequences of the peaks were extracted from the *Arabidopsis thaliana* genome as a FASTA file by Bedtools (Quinlan and Hall, 2010). To identify the candidates of NPR1 binding motifs, the FASTA files were subjected to MEME (Multiple EM for Motif Elicitation)-ChIP with the default parameter (–meme-minw 6–meme-maxw 10) (Ma et al., 2014; Machanick and Bailey, 2011) and generated a density plot of the distribution of the motifs.

ChIP-seq data of MYC2 (CRR032460) and MED25 (CRR032462) were downloaded from the website of the Genome Sequence Archive (Wang et al., 2019), and TDF files were generated as described above to visualize sequence reads by IGV.

Agrobacterium-Mediated Transient Assay in N. benthamiana Leaves

Binary plant transformation vectors pGWB635, pGWB605, and pGWB611 were kindly provided by Dr. Tsuyoshi Nakagawa (Nakamura et al., 2010). The *LOX3* promoter in pDONR221 was cloned into pGWB635 by LR clonase reaction (Gateway® LR Clonase Enzyme mix, Invitrogen). The *MYC2-GFP*, *GFP*, *MED25-GFP*, *NPR1-FLAG*, *npr1*^{H334Y}*-FLAG*, and *JAZ1-FLAG* in pGWB605 and pGWB611 amplified by gene specific primers (Table S3) were cloned into the mannopine synthase (mas) promoter-driven pPZP200 using the SwaI restriction enzyme. These constructs were transformed into *A. tumefaciens* strain GV3101 as described above (Matsushita, 2011). After infiltration of transformed *Agrobacterium*, *N. benthamiana* was placed under a 16 h light and 8 h dark cycle at 25°C for 48 h. The infiltrated leaves were harvested and stored at −80°C until use. The activities of the luciferase were measured using the Dual-Luciferase® Reporter Assay System (Promega). Frozen samples were ground to a fine powder by Geno/Grinder® 2000 (SPEX, NJ, USA) and mixed with 500 μL of Passive Lysis Buffer per 10 mg of sample weight. After centrifugation at 12,000 rpm at 4°C for 10 min, 10 μL of supernatant was mixed with 90 μL of Passive Lysis Buffer. 10 μL of diluted sample was mixed with 50 μL of the Luciferase Assay Reagent II in 96-well plates and detected by a Spark 10M Multimode Microplate Reader (TECAN).

QUANTIFICATION AND STATISTICAL ANALYSIS

Statistical analyses were performed using the one-way or two-way analysis of variance (ANOVA). Statistical details are reported in the figure legends. Data are shown as mean ± SD or ± SEM n represents the sample number.

Cell Reports, Volume *37*

Supplemental information

Suppression of MYC transcription activators by the immune cofactor NPR1 fine-tunes plant immune responses

Mika Nomoto, Michael J. Skelly, Tomotaka Itaya, Tsuyoshi Mori, Takamasa Suzuki, Tomonao Matsushita, Mutsutomo Tokizawa, Keiko Kuwata, Hitoshi Mori, Yoshiharu Y. Yamamoto, Tetsuya Higashiyama, Hironaka Tsukagoshi, Steven H. Spoel, and Yasuomi Tada

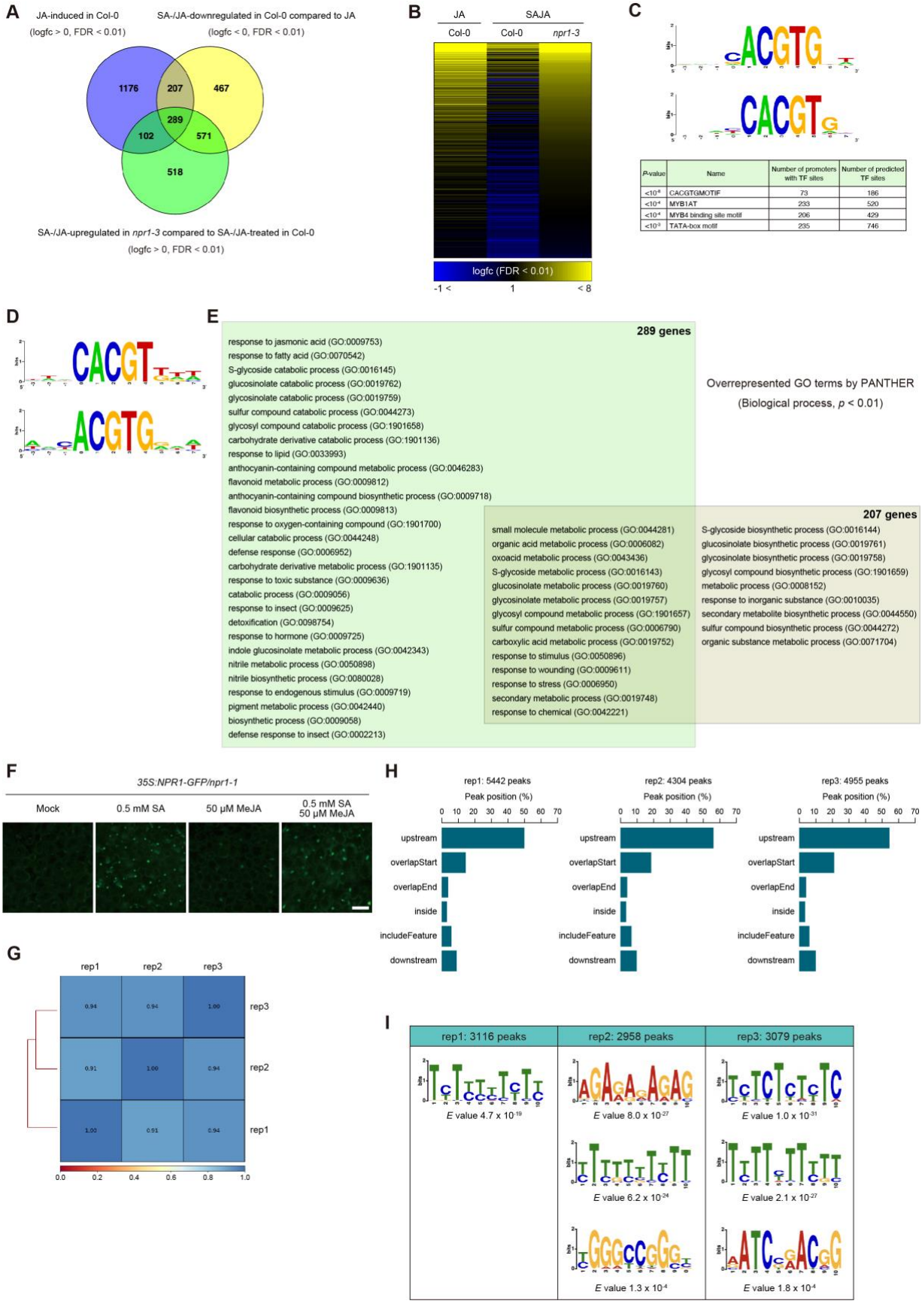
A
JA-induced in Col-0
(logfc > 0, FDR < 0.01)
SA-/JA-downregulated in Col-0 compared to JA
(logfc < 0, FDR < 0.01)
1176
207
467
289
102
571
518
SA-/JA-upregulated in npr1-3 compared to SA-/JA-treated in Col-0
(logfc > 0, FDR < 0.01)
B
JA
SAJA
Col-0
Col-0
npr1-3
logfc (FDR < 0.01)
-1 <
1
< 8
C
P-value
Name
Number of promoters with TF sites
Number of predicted TF sites
<10-6
CACGTGMOTIF
73
186
<10-4
MYB1AT
233
520
<10-4
MYB4 binding site motif
206
429
<10-3
TATA-box motif
235
746
D
E
289 genes
response to jasmonic acid (GO:0009753)
response to fatty acid (GO:0070542)
S-glycoside catabolic process (GO:0016145)
glucosinolate catabolic process (GO:0019762)
glycosinolate catabolic process (GO:0019759)
sulfur compound catabolic process (GO:0044273)
glycosyl compound catabolic process (GO:1901658)
carbohydrate derivative catabolic process (GO:1901136)
response to lipid (GO:0033993)
anthocyanin-containing compound metabolic process (GO:0046283)
flavonoid metabolic process (GO:0009812)
anthocyanin-containing compound biosynthetic process (GO:0009718)
flavonoid biosynthetic process (GO:0009813)
response to oxygen-containing compound (GO:1901700)
cellular catabolic process (GO:0044248)
defense response (GO:0006952)
carbohydrate derivative metabolic process (GO:1901135)
response to toxic substance (GO:0009636)
catabolic process (GO:0009056)
response to insect (GO:0009625)
detoxification (GO:0098754)
response to hormone (GO:0009725)
indole glucosinolate metabolic process (GO:0042343)
nitrile metabolic process (GO:0050898)
nitrile biosynthetic process (GO:0080028)
response to endogenous stimulus (GO:0009719)
pigment metabolic process (GO:0042440)
biosynthetic process (GO:0009058)
defense response to insect (GO:0002213)
Overrepresented GO terms by PANTHER
(Biological process, p < 0.01)
207 genes
small molecule metabolic process (GO:0044281)
organic acid metabolic process (GO:0006082)
oxoacid metabolic process (GO:0043436)
S-glycoside metabolic process (GO:0016143)
glucosinolate metabolic process (GO:0019760)
glycosinolate metabolic process (GO:0019757)
glycosyl compound metabolic process (GO:1901657)
sulfur compound metabolic process (GO:0006790)
carboxylic acid metabolic process (GO:0019752)
response to stimulus (GO:0050896)
response to wounding (GO:0009611)
response to stress (GO:0006950)
secondary metabolic process (GO:0019748)
response to chemical (GO:0042221)
S-glycoside biosynthetic process (GO:0016144)
glucosinolate biosynthetic process (GO:0019761)
glycosinolate biosynthetic process (GO:0019758)
glycosyl compound biosynthetic process (GO:1901659)
metabolic process (GO:0008152)
response to inorganic substance (GO:0010035)
secondary metabolite biosynthetic process (GO:0044550)
sulfur compound biosynthetic process (GO:0044272)
organic substance metabolic process (GO:0071704)
F
35S:NPR1-GFP/npr1-1
Mock
0.5 mM SA
50 μM MeJA
0.5 mM SA
50 μM MeJA
G
rep1
rep2
rep3
0.94
0.94
1.00
0.91
1.00
0.94
1.00
0.91
0.94
0.0
0.2
0.4
0.6
0.8
1.0
H
rep1: 5442 peaks
rep2: 4304 peaks
rep3: 4955 peaks
Peak position (%)
0 10 20 30 40 50 60 70
upstream
overlapStart
overlapEnd
inside
includeFeature
downstream
I
rep1: 3116 peaks
rep2: 2958 peaks
rep3: 3079 peaks
E value 4.7 x 10-19
E value 8.0 x 10-27
E value 1.0 x 10-31
E value 6.2 x 10-24
E value 2.1 x 10-27
E value 1.3 x 10-4
E value 1.8 x 10-4

Figure S1. NPR1 is distributed to the promoter regions of JA-responsive genes. Related to Figure 1.

(A) Two-week-old seedlings were treated with MeJA (50 μM) or both MeJA and SA (0.5 mM) and analyzed by RNA-seq. Venn diagram represents 289 JA-responsive genes differentially downregulated in a SA/NPR1-dependent manner.

(B) The 289 NPR1-suppressed genes are shown in descending order of expression levels. Color scale represents $\log_2$ fold-change values of differentially expressed genes compared to mock-treated wild type (FDR < 0.01).

(C) The overrepresented octamer sequences in the 289 NPR1-suppressed gene promoters were aligned and subjected to Weblogo (http://weblogo.berkeley.edu/logo.cgi). The Y-axis indicates the relative frequency and sequence conservation. Athena analysis was performed to identify the enriched *cis*-regulatory elements on the 289 JA-responsive genes, which were downregulated in a SA/NPR1-dependent manner.

(D) The overrepresented octamer sequences in the 207 non-antagonized JA-responsive gene promoters were aligned and subjected to Weblogo (http://weblogo.berkeley.edu/logo.cgi). The Y-axis indicates the relative frequency and sequence conservation.

(E) Enriched GO terms derived from 289 and 207 genes by the PANTHER classification system (Table S1; $P < 0.01$).

(F) Two-week-old *35S:NPR1-GFP* seedlings were treated with water, 0.5 mM SA, 50 μM MeJA, or both 0.5 mM SA and 50 μM MeJA for 6 hr. Leaf tissue was examined using fluorescence microscopy. Scale bars, 50 μm.

(G) Correlation matrix of the read coverages between three biological replicates.

(H) Position of the peaks relative to the annotated nearest TSS. upstream, peak resides upstream of the feature; overlapStart, peak overlaps with the start of the feature; overlapEnd, peak overlaps with the end of the feature; inside, peak resides inside the feature; includeFeature, peak includes the feature entirely; downstream, peak resides downstream of the feature.

(I) NPR1-binding motifs were identified de novo using MEME-ChIP with corresponding *E* value in 2,554 genes. The *E* value is an estimate of the expected number of motifs that can be found in a similarly sized set of random sequences.

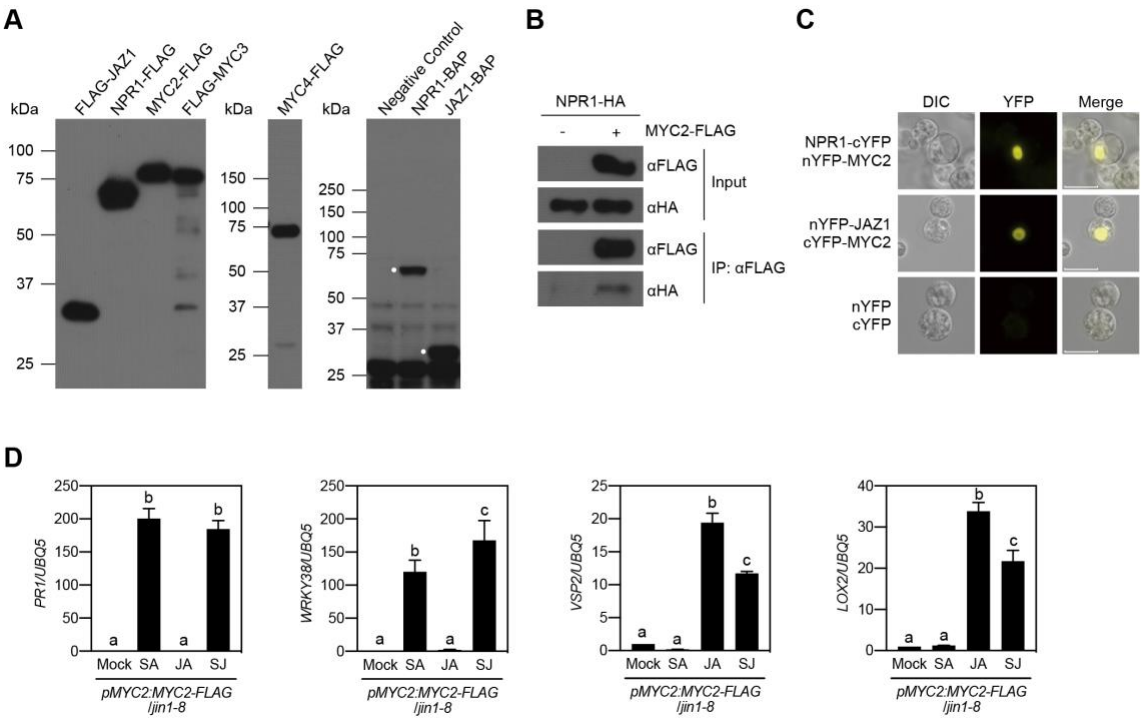

Figure S2. NPR1 directly associates with MYC2. Related to Figure 2.

(A) In vitro-synthesized recombinant proteins (1 μl) were subjected to Western blotting with an anti-FLAG antibody or biotin-HRP. White dots indicate target proteins.

(B) In vitro pull-down assays of NPR1-HA with MYC2-FLAG. Proteins were incubated at 16°C for 3 hr, followed by pull-down with an anti-FLAG antibody and immunoblotting analysis with anti-FLAG and anti-HA antibodies.

(C) BiFC analysis 12 hr after transfection of protoplast cells with *NPR1-cYFP*, *nYFP-JAZ1*, *nYFP-MYC2*, or *cYFP-MYC2*. Transfection with *nYFP* and *cYFP* served as negative controls. Bright field (DIC), YFP images, and merged pictures (Merge) are shown. Scale bars, 25 μm.

(D) Two-week-old *pMYC2:MYC2-FLAG/jin1-8* seedlings were pretreated with water (Mock) or 0.5 mM SA for 12 hr, followed by treatment with water, 0.5 mM SA, 50 μM MeJA, or both 0.5 mM SA and 50 μM MeJA for 4 hr. Expression of *PR1*, *WRKY38*, *VSP2*, and *LOX2* was determined by qPCR and normalized with *UBQ5*. Error bars represent SD (n = 3). Letters indicate statistically significant differences (one-way ANOVA, $P < 0.05$).

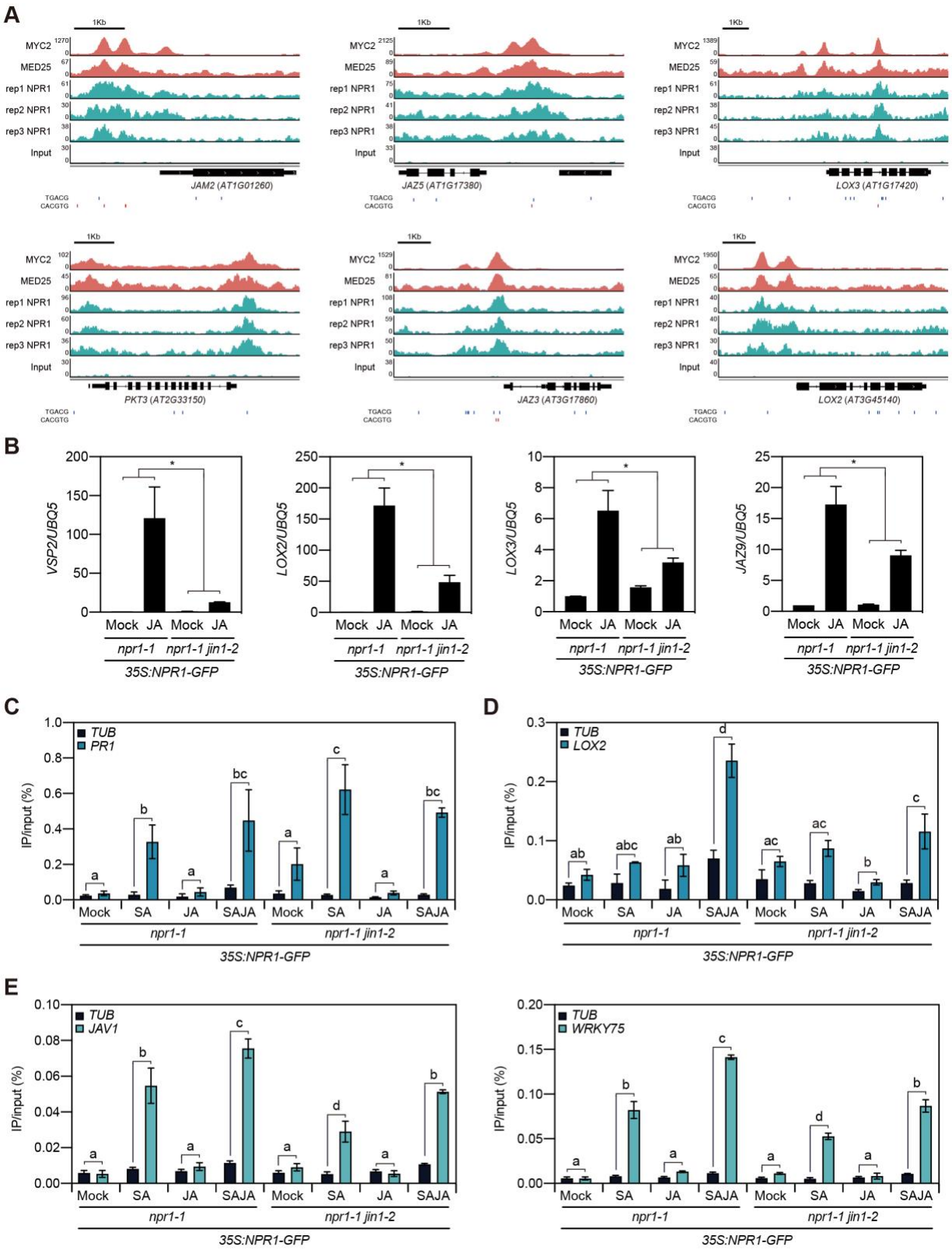
A
1Kb
MYC2
MED25
rep1 NPR1
rep2 NPR1
rep3 NPR1
Input
JAM2 (AT1G01260)
JAZ5 (AT1G17380)
LOX3 (AT1G17420)
PKT3 (AT2G33150)
JAZ3 (AT3G17860)
LOX2 (AT3G45140)
TGACG
CACGTG
B
VSP2/UBQ5
LOX2/UBQ5
LOX3/UBQ5
JAZ9/UBQ5
Mock JA Mock JA
npr1-1 npr1-1 jin1-2
35S:NPR1-GFP
C
TUB
PR1
IP/input (%)
Mock SA JA SAJA Mock SA JA SAJA
npr1-1
npr1-1 jin1-2
35S:NPR1-GFP
D
TUB
LOX2
E
TUB
JAV1
TUB
WRKY75

Figure S3. Known JA-responsive genes were identified as target genes of NPR1 and MYC2/MED25. Related to Figure 3.

(A) Co-occupancy of NPR1 and MYC2/MED25 on the JA-responsive *JAM2*, *JAZ5*, *LOX3*, *PKT3*, *JAZ3*, and *LOX2* promoters obtained from 1,137 NPR1/MYC2/MED25-targeted genes as shown in Figure 3E. Blue and red lines indicate the TGACG and CACGTG (G-box) motifs, respectively.

(B) Two-week-old seedlings of *35S:NPR1-GFP* in *npr1-1* and *npr1-1 jin1-2* backgrounds were treated with water (Mock) or 50 μM MeJA for 6 hr. Expression of *VSP2*, *LOX2*, *LOX3*, and *JAZ9* was determined by qPCR and normalized with *UBQ5*. Error bars represent SD (n = 3). Asterisks indicate significant difference (two-way ANOVA; **P* < 0.001).

(C and D) ChIP-qPCR analyses of NPR1-GFP binding to the G-box from SA-responsive *pPR1* and *pLOX2*. Two-week-old seedlings of *35S:NPR1-GFP* in *npr1-1* and *npr1-1 jin1-2* plants were treated with water (Mock), 0.5 mM SA, 50 μM MeJA, or both 0.5 mM SA and 50 μM MeJA for 6 hr. Error bars represent SD (n = 3). Letters indicate statistically significant differences (two-way ANOVA, *P* < 0.05).

(E) ChIP-qPCR analyses of NPR1-GFP binding to the JA-responsive *pJAV1* and *pWRKY75*. Two-week-old seedlings of *35S:NPR1-GFP* in *npr1-1* and *npr1-1 jin1-2* plants were treated as described in (C). Error bars represent SD (n = 3). Letters indicate statistically significant differences (one-way ANOVA, *P* < 0.05).

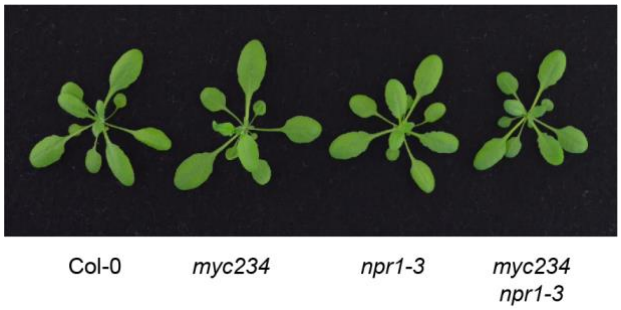

Figure S4. Photograph of 4-week-old Col-0, *myc234*, *npr1-3*, and *myc234 npr1-3* plants. Related to Figure 4.

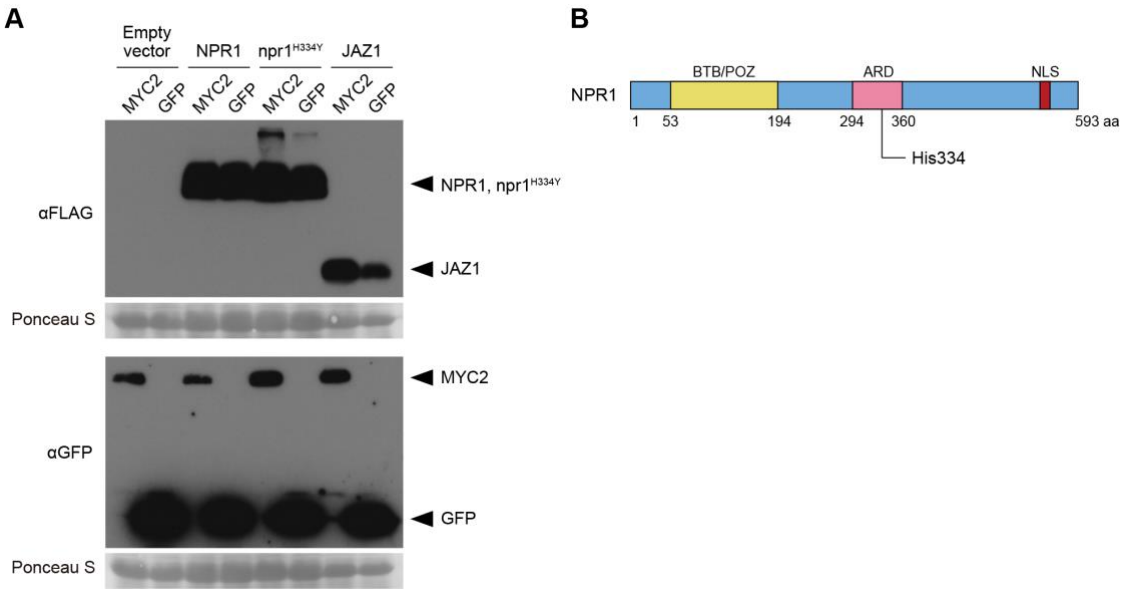

Figure S5. Effectors used for the reporter assay. Related to Figure 5.

(A) Total protein was extracted from *Agrobacterium*-infected *N. benthamiana* leaves (Figure 5B) and subjected to SDS-PAGE and Western blotting using anti-FLAG and anti-GFP antibodies. Ponceau S staining served as a loading control.

(B) Schematic representation of protein structural domains. BTB/POZ, Broad Complex, Tramtrack, Bric-à-brac/Pox virus, and Zinc finger; ARD, ankyrin repeats domain; NLS, nuclear localization signal.

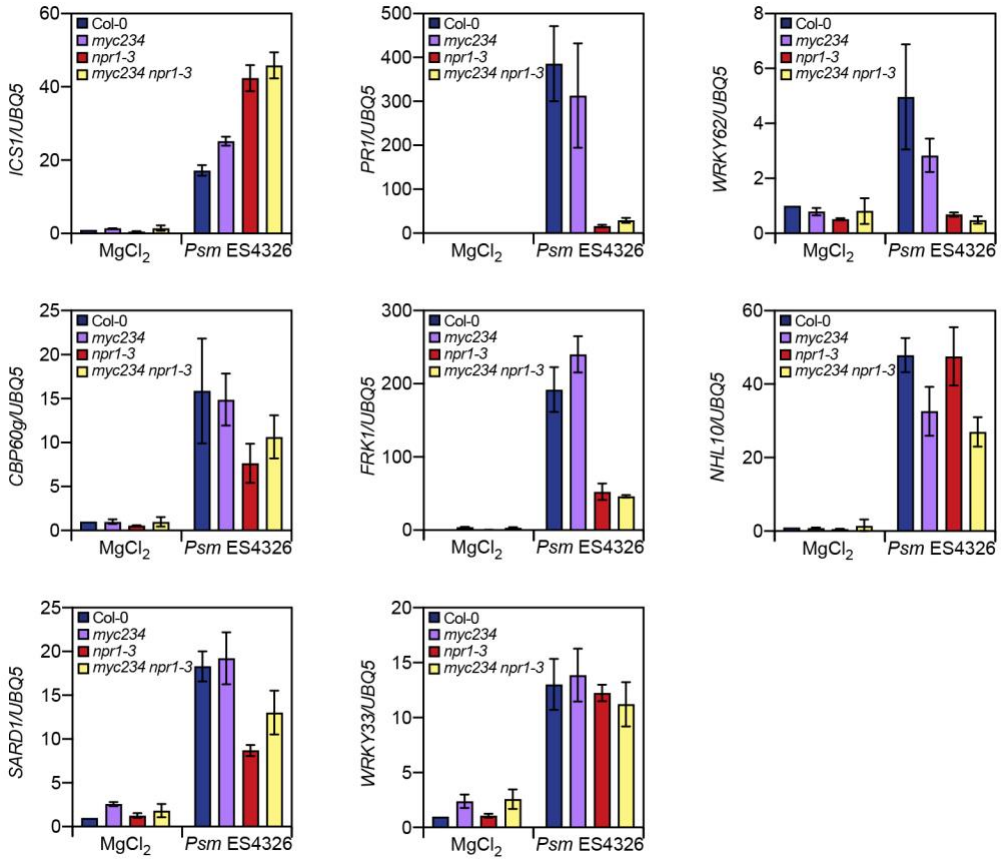

Figure S6. Expression analysis of defense-related genes in *myc234 npr1-3* plants. Related to Figure 6.

Expression of defense-related genes as shown in Figure 6B. Leaves were inoculated with 10 mM $MgCl_2$ or *Psm* ES4326 (OD_{600} = 0.001) for 24 hr then analyzed for the expression of the SA biosynthetic enzyme *ICS1*, the SA-responsive *PR1* and *WRKY62*, PTI-responsive *CBP60g*, *FRK1*, *NHL10*, *SARD1*, and *WRKY33* by qPCR and normalized with *UBQ5*. Error bars represent SD (n = 3).

Table S3. Primers used in this study. Related to STAR methods.

Primer name	Sequence (5' to 3')	Source
Primers for Genotyping		
jin1-8_SALK_061267-F	CTCGAGCTGGTTCTTGATTTG	(Hou et al., 2010)
jin1-8_SALK_061267-R	TGGTTTTTCTTGGTTTCGATG	
pMYC2:MYC2-FLAG-F	AATCTGCAGCTCTCTTTCAACAAGGTGATAG	
pMYC2:MYC2-FLAG-R	AAAGGTACCGATTTTTGAAATCAAACTTGC	
myc3_GK445B11-F	ATCGGAAAAGAGTAATACGTGAGC	(Kleinboelting et al., 2012)
myc4_GK491E10-F	GCATTTCCCGCTTCTTTATTC	
o8474	ATAATAACGCTGCGGACATCTACATTTT	
Primers for BP Gateway cloning		
MYC2 -F	GGGGACAAGTTTGTACAAAAAAGCAGGCTCTATGACTGATTACCGGCTA	This study
MYC2 -R	GGGGACCACTTTGTACAAGAAAGCTGGGTAACCGATTTTTGAAATCAA	
MYC3 -F	GGGGACAAGTTTGTACAAAAAAGCAGGCTCTATGAACGGCACAACATCA	
MYC3 -R	GGGGACCACTTTGTACAAGAAAGCTGGGTAATAGTTTTCTCCGACTTTCGTC	
MYC4 -F	GGGGACAAGTTTGTACAAAAAAGCAGGCTCTATGTCTCCGACGAATGTTC	
MYC4 -R	GGGGACCACTTTGTACAAGAAAGCTGGGTATGGACATTCTCCAACTTTCTC	
NPR1 -F	GGGGACAAGTTTGTACAAAAAAGCAGGCTCTATGGACACCACCATTGAT	
NPR1 -R	GGGGACCACTTTGTACAAGAAAGCTGGGTACCGACGACGATGAGAGAG	
JAZ1-F	GGGGACAAGTTTGTACAAAAAAGCAGGCTCTATGTCGAGTTCTATGGAA	
JAZ1-R	GGGGACCACTTTGTACAAGAAAGCTGGGTATATTTCAGCTGCTAAACC	
pLOX3-F	GGGGACAAGTTTGTACAAAAAAGCAGGCTCTGTCATAAATTTTAAATTTAGATG	
pLOX3-R	GGGGACCACTTTGTACAAGAAAGCTGGGTACACGATAATCTAATAAATTACAA	
Primers for in vitro protein synthesis		
JAZ1-CF	CACAAAACATTTCCCTACATACAACTTTCAACTTCCTATTATGTCGAGTTCTATGGAA	This study
JAZ1-CR	AGTACCTCCCTGCTGGAGACCTATTTCAGCTGCTAAACC	
MYC2-CF	CACAAAACATTTCCCTACATACAACTTTCAACTTCCTATTATGACTGATTACCGGCTA	
ΔNMYC2-CF	CACAAAACATTTCCCTACATACAACTTTCAACTTCCTATTATGGGATTAGCTGGTAAAGCG	
MYC2-CR	AGTACCTCCCTGCTGGAGACCACCGATTTTTGAAATCAA	
MYC4-CF	CACAAAACATTTCCCTACATACAACTTTCAACTTCCTATTATGTCTCCGACGAATGTT	
MYC4-CR	AGTACCTCCCTGCTGGAGACCTGGACATTCTCCAACTTT	
NPR1-CF	CACAAAACATTTCCCTACATACAACTTTCAACTTCCTATTATGGACACCACCATTGAT	
NPR1-CF	AGTACCTCCCTGCTGGAGACCCCGACGACGATGAGAGAG	

JAZ1-NF	CCAGCAGGGAGGTACTATGTCGAGTTCTATGGAA	
JAZ1-NR	CCTTATGGCCGGATCCAAGAGCTCTTTTTTTTTTTTTATATTTCAGCTGCTAAACC	
MYC3-NF	CCAGCAGGGAGGTACTATGAACGGCACAACATCATC	
MYC3-NR	CCTTATGGCCGGATCCAAGAGCTCTTTTTTTTTTTTTAATAGTTTTCTCCGACTTTCGTC	
Primers for mutated MYC2 and NPR1		
NPR1_H334Y_mut-F	GTGCTTTATGTTGCTGCGATGCGGAAG	This study
NPR1_H334Y_mut-R	AGCAACATAAAGCACCGTATATCCCCT	
Primers for RT-qPCR		
UBQ5-F	GACGCTTCATCTCGTCC	(Kesarwani et al., 2007)
UBQ5-R	GTAAACGTAGGTGAGTCCA	
PR1-F	CTCATACACTCTGGTGGG	
PR1-R	TTGGCACATCCGAGTC	
ICS1-F	GGCAGGGAGACTTACG	(Jiang et al., 2013)
ICS1-R	AGGTCCCGCATACATT	
WRKY62-F	GAGAGCTCCAGGAAACCAC-	This study
WRKY62-R	CTTTGATCTGCTTTTGTCCG	
VSP2-F	GCTGGCGTGACCTACTGGAA	
VSP2-R	TCTTCACGAGACTCTTCCTCACC	
LOX2-F	CGTCATGCTGGCTATGGAAT	
LOX2-R	GTACAGGCATGAGTCCTCAA	
NHL10-F	CCAAAACCTTGTTATTTTTAACG	
NHL10-R	AACAGTGGAGGTAGTTGTAGTTCC	
WRKY33-F	CTGAAGCAAAGAGATGGAAAG	
WRKY33-R	CTTGTAGTAGCTTCTTGGATTTGG	
CBP60g-F	CGGGCGTAACACTTCTCTTC	
CBP60g-R	AGCTTCGGCCTTTAATTGGT	
SARD1-F	CCTCAACCAGCCCTACGTTA	
SARD1-R	TAGTGGCTCGCAGCATATTG	
FRK1-F	CCTAGAGTCGTTTCACTAAATATATC	
FRK1-R	GTATTACCGGATAAATCTAATTTTC	
LOX3-F	CCCTGCCGATCTAATTCGC	
LOX3-R	CGTTCAACATAGGTTCGGACC	
JAZ9-F	AAGCTCTGCCACTCACACTG	
JAZ9-R	CTCTTTGCGCTTCTCCAAG	
JAZ8-F	ATGTTACCCATCTTCAGGC	(Pandey et al., 2010)
JAZ8-R	CTTTTGGATTTGGAAGCTGA	
JAZ10-F	CGAGTCGTCGATGGAGACAG	
JAZ10-R	CTCGAGAAAACGTTGCAGTG	
ANAC019-F	GCATCTCGTCGCTCAG	(Zheng et al., 2012)

ANAC019-R	CTCGACTTCCTCCTCCG	
ANAC055-F	GCGCTGCCTCATAGTC	
ANAC055-R	CGAGGAATCCCCTCAGT	
ANAC072-F	TGGGTGTTGTGTCGAAT	
ANAC072-R	ATCGTAACCACCGTAACT	
Primers for ChIP-qPCR		
TUB-F	ATCCGTGAAGAGTACCCAGAT	(Hou et al., 2010)
TUB-R	AAGAACCATGCACTCATCAGC	
LOX4-F	TGTTGGAAAGTTACCTTACG	
LOX4-R	TTGTTACTTGTTTTTCTTTCG	
PR1-as-1-For (JMS178)	CGGTCACCTAGAGTTTTTCAA	(Saleh et al., 2015)
PR1-as-1-Rev (JMS179)	CCGCCACATCTATGACGTAAG	
JAZ6-F	TGCATGAAATAAGGTTGGTACCG	(Chen et al., 2012)
JAZ6-R	TCGGCTGCGATGGCTAATAC	
JAZ8-F	ACAAATCCAAAAGGACCAA	
JAZ8-R	GTATATGGATTGAGATTATGTTGAT	
LOX2-F	CTTTAGATACAGTGGTCCTCC	This study
LOX2-R	GGTACTCTACGACGTTAATGTC	
JAZ9-F	GACTTGCGTCTGTTTGAAAC	
JAZ9-R	CTAAGCTCATTTCATAACACGTG	
JRG21-F	GTAAATATCACGTGGAGGGG	
JRG21-R	TTCTTTCCAATTACGCATTAAC	
JAV1-F	GTCAGCTTTGTGACGATTATG	
JAV1-R	CTTTCCCAACAAGTTGACG	
WRKY75-F	CGTAACACGTACACGACG	
WRKY75-R	CTGACGTAAGAATCAATTACTCAC	
LOX3-F	GACGGCAAGGGTTCCTTC	
LOX3-R	TTTAGCTAAGGCCATCACGATAATC	
Primers for transient transactivation assays		
pMAS:MYC2-GFP-F	ATAAGAGCTCTATTTATGACTGATTACCGGCTAC	This study
pMAS:NPR1-FLAG-F	ATAAGAGCTCTATTTATGGACACCACCATTGATG	
pMAS:NPR1-FLAG-R	TCTAGCCATGGATTTTCACTTGTCATCGTCATCCTTG	
pMAS:JAZ1-FLAG-F	ATAAGAGCTCTATTTATGTCGAGTTCTATGGAATG	
pMAS:MED25-GFP-F	ATAAGAGCTCTATTTATGTCGTCGGAGGTGAAACA	
pMAS:GFP-F	ATAAGAGCTCTATTTATGGTGAGCAAGGGCGAG	
pMAS:GFP-R	TCTAGCCATGGATTTTTACTTGTACAGCTCGTC	
pLOX3:fLUC-F	GGGGACAAGTTTGTACAAAAAAGCAGGCTCTGTCATAA ATTTTAAATTTAGATG	
pLOX3:fLUC-R	GGGGACCACTTTGTACAAGAAAGCTGGGTACACGATAA TCTAATAAATTACAA	